

Accepted Manuscript

Journal of the Geological Society

Paleogene drainage system evolution in the NE Faroe-Shetland Basin

Faye Walker, Nick Schofield, John Millett, David Jolley, Sverre Planke & Simon Holford

DOI: <https://doi.org/10.1144/jgs2021-121>

To access the most recent version of this article, please click the DOI URL in the line above. When citing this article please include the above DOI.

Received 1 October 2021

Revised 25 April 2022

Accepted 6 May 2022

© 2022 The Author(s). Published by The Geological Society of London. All rights reserved. For permissions: <http://www.geolsoc.org.uk/permissions>. Publishing disclaimer: www.geolsoc.org.uk/pub_ethics

Manuscript version: Accepted Manuscript

This is a PDF of an unedited manuscript that has been accepted for publication. The manuscript will undergo copyediting, typesetting and correction before it is published in its final form. Please note that during the production process errors may be discovered which could affect the content, and all legal disclaimers that apply to the journal pertain.

Although reasonable efforts have been made to obtain all necessary permissions from third parties to include their copyrighted content within this article, their full citation and copyright line may not be present in this Accepted Manuscript version. Before using any content from this article, please refer to the Version of Record once published for full citation and copyright details, as permissions may be required.

Paleogene drainage system evolution in the NE Faroe-Shetland Basin

Faye Walker¹, Nick Schofield¹, John Millett^{1,2}, David Jolley¹, Sverre Planke², Simon Holford³

1. Geology and Petroleum Geology, School of Geosciences, University of Aberdeen, Aberdeen, UK
2. VBPR AS, Oslo, Norway
3. Australian School of Petroleum and Energy Resources, University of Adelaide, Adelaide SA 5000, Australia

Abstract

Incised drainage systems can provide a record of the timing, duration and magnitude of ancient vertical crustal motions. The NE Atlantic underwent rapid uplift ~56 Ma, resulting in widespread incision and the formation of Paleogene unconformities across the Faroe-Shetland Basin. This study uses 3D seismic data to map a newly-identified incised drainage system in the northern Faroe-Shetland Basin that formed during this uplift, and compare it to similar incision surfaces in the region. The ~30x50 km erosional surface is a composite feature, comprising the Upper Thanetian Unconformity, which was rejuvenated and eroded by the younger Flett Unconformity, and records prolonged regional uplift during the late Thanetian-earliest Ypresian punctuated by a phase of subsidence. The drainage system was influenced by igneous intrusions resulting in diversion of channels around forced fold structures. Several preserved paleoshorelines occur close to the basinward limit of the incision surface, recording progressive backstepping of the shoreline and marine transgression during early Ypresian subsidence. The drainage system may have supplied 'clean' sand, eroded from the North Shetland Platform, to the Flett Sub-basin, with the potential to form high-quality reservoir units. Such sands may have been concentrated along shorelines coeval with the drainage system, but potentially were also delivered further out into the basin.

Introduction

Incision of drainage systems occurs in response to a fall in base level, whether due to global (eustatic) sea level fall or uplift of the earth's surface (e.g. Posamentier and Vail 1988; Schumm 1993), with incision being influenced by factors such as stream power, sediment influx and bedrock geology. By accounting for eustatic sea level changes, the evolution of ancient drainage systems can provide valuable insights into the timing and magnitude of vertical crustal motions and the mechanisms responsible such as compressional or flexural tectonic forces, thermal or dynamic effects from the mantle or igneous underplating of the crust (Sleep 1990; Boldreel and Andersen 1993; Clift and Turner 1998; Clift 1999; Praeg *et al.* 2005). In addition, aside from the usefulness for the reconstruction of crustal movements, ancient drainage systems are also of importance for hydrocarbon exploration and CO₂ sequestration, as they allow tracing of source-to-sink sedimentation. When incision has taken place into quartz-rich source regions (e.g. granites or older sandstones) drainage systems track sediment transport pathways from proximal to distal depositional environments which can result in the accumulation of high-quality reservoirs.

Paleocene-Eocene-aged unconformities and incised drainage systems have been documented in the Faroe-Shetland Basin (Smallwood and Gill 2002; Shaw Champion *et al.* 2008; Hartley *et al.* 2011; Hardman *et al.* 2018b; Jolley *et al.* 2021) and North Sea (Underhill 2001; Stucky de Quay *et al.* 2017). These incised drainage systems record transient uplift events in the NE Atlantic region which have been attributed to variations in the amount of thermal support provided by pulsing of the proto-Iceland Plume (Rudge *et al.* 2008; Hartley *et al.* 2011; Conway-Jones and White 2020). This hypothesis predicts that the transient uplift events recorded at the surface result from the rising and radial spreading-out of hotter than ambient mantle pulses

beneath the lithosphere (Parnell-Turner *et al.* 2014), though we note that tectonic processes associated with continental breakup have also been invoked to explain the surface uplift and subsidence record (Stoker *et al.* 2017).

This study utilises high-quality 3D seismic and released well data to map newly-identified Thanetian-Ypresian incision surfaces in the NE Faroe-Shetland Basin, in order to investigate the Paleocene-Eocene evolution of the basin. We examine the extrinsic geological factors controlling the extent and distribution of the drainage system, including both basin structure and volcanism, and discuss the potential implications for hydrocarbon prospectivity in the region.

Geological Setting and Tectonic History

The Faroe-Shetland Basin (FSB), located between the Faroe and Shetland Islands (Fig. 1), is one of several NE-SW trending basins along the NE Atlantic Margin. It comprises numerous sub-basins which also trend NE-SW, with this orientation thought to have been inherited from the underlying Caledonian structural fabric (Ritchie *et al.* 2011; Schöpfer and Hinsch 2019). The sub-basins are separated by Precambrian crystalline basement highs (Holdsworth *et al.* 2019), often capped by Paleozoic-Mesozoic sedimentary rocks, and the basin-fill comprises a variety of (often heavily-intruded) Mesozoic-Recent sedimentary strata and extrusive volcanics (Lamers and Carmichael 1999; Ritchie *et al.* 2011; Jolley *et al.* 2021).

The FSB has had a long and complex tectonic evolution, thought to begin with the collapse of the Caledonian Orogeny in Devonian-Carboniferous times. Subsequently the region has largely been dominated by rifting, with several phases of extension occurring from the Permo-Triassic to the Paleocene (Ziegler 1988; Doré *et al.* 1999). These phases of extension were punctuated by periods of uplift and inversion around the Carboniferous-Permian boundary

(Variscan Orogeny; Roberts *et al.* 1999), at the end of the Cretaceous (Roberts *et al.* 1999; Ritchie *et al.* 2011), and from the Eocene onwards (Ritchie *et al.* 2008; Ellis and Stoker 2014). The main phase of rifting responsible for much of the present day structural geometry of the FSB is thought to have occurred during the Cretaceous (Doré *et al.* 1997; Lamers and Carmichael 1999; Ritchie *et al.* 2011), although potentially beginning as early as the Jurassic (Haszeldine *et al.* 1987; Coward *et al.* 2003; Schöpfer and Hinsch 2019). Seafloor spreading began in the North Atlantic at ~55-54 Ma (Ritchie *et al.* 2011; Ellis and Stoker 2014), and was immediately preceded by rifting associated with intense magmatism resulting in emplacement of the North Atlantic Igneous Province (NAIP). Regional uplift occurred during the Danian (Jolley and Bell 2002b), which is often attributed to the initiation of the proto-Iceland Plume (e.g. White, 1989; White and McKenzie, 1989; Saunders *et al.*, 1997; Hansen *et al.*, 2009; Hardman *et al.*, 2018). The remainder of the Cenozoic, from the early Eocene to the present day, involved regional post-rift thermal subsidence punctuated by pulses of compression, resulting in localized uplift and erosion (Roberts 1989; Boldreel and Andersen 1993; Doré *et al.* 1999; Tassone *et al.*, 2014; Kimbell *et al.* 2017).

Lower Paleogene Sedimentary Succession

The Lower Paleogene succession in the FSB is subdivided into five main stratigraphic units: the Sullom (oldest), Vaila, Lamba, Flett, and Balder formations (youngest) (Fig. 2). For consistency with previous work in the FSB, this study utilizes the lithostratigraphic nomenclature presented in Ritchie *et al.* (2011) and Stoker & Varming (2011), and the T-sequence framework devised by Ebdon *et al.* (1995). Ages for the various stratigraphic units are taken from Jolley *et al.* (2021) (Fig. 2).

The Sullom Fm. was deposited during the Danian (sequence T10-T22). It typically comprises slope and basinal mudstones, with thin shelf deposits and submarine fan sandstones around the basin margins, and reaches thicknesses of up to ~1 km in the Flett sub-basin (Knox *et al.* 1997; Ritchie *et al.* 2011; Mudge 2015). The sediments were derived primarily from the West Shetland Platform (WSP), with minor input from east Greenland (Morton *et al.* 2002; Jolley and Morton 2007).

The Vaila Fm. is Selandian in age (sequence T22-T35). It attains thicknesses of ~600-1000 m in the southern and central FSB (e.g. in 214/27-2), and thins northwards to ~200 m in parts of the Flett sub-basin and Møre Basin (Knox *et al.* 1997; Mudge 2015). It comprises mainly deep-marine mudstones with significant sequences of submarine fan sandstones in the eastern part of the FSB, supplied from both the WSP and east Greenland (Knox *et al.* 1997; Lamers and Carmichael 1999; Morton *et al.* 2002; Jolley and Morton 2007; Mudge 2015).

The Lamba Fm. is Thanetian in age (sequence T36-T38) and comprises mudstones and subordinate sandstones deposited in basin and slope environments in the eastern part of the FSB, along with shelf sediments on both margins (Knox *et al.* 1997; Mudge 2015). It was deposited as a progradational package primarily building out from the SE to the NW and is up to ~720 m thick in 208/17-1 (Knox *et al.* 1997; Jolley and Morton 2007; Shaw Champion *et al.* 2008; Mudge 2015).

The Flett Fm. was deposited during the Thanetian-Ypresian (sequence T40-T45) in environments ranging from terrestrial (including fluvial) to basin slope. It comprises a variety of sandstones and mudstones and has a maximum thickness of ~860 m found in 206/2-1a (Knox *et al.* 1997; Mudge and Bujak 2001; Mudge 2015). It was largely deposited beyond the shelf edge of the Lamba Fm., resulting in bypass, erosion and non-deposition along the southern margin of the

FSB, along with regional incised unconformity surfaces at the base and top of sequence T40 (Smallwood and Gill 2002; Shaw Champion *et al.* 2008; Hartley *et al.* 2011; Ritchie *et al.* 2011; Jolley *et al.* 2021). The Flett Fm. contains two important reservoir units: the terrestrial to shallow marine Colsay Sandstone Mb., which forms the main reservoir in the Rosebank field (Knox *et al.* 1997; Schofield and Jolley 2013; Hardman *et al.* 2018a); and the marine Hildasay Mb., which is the primary reservoir in the Cambo field (Knox *et al.* 1997; Mudge and Bujak 2001; Mudge 2015).

The Balder Fm. was deposited during the Ypresian (sequence T50). To the north (e.g. Erlend Sub-basin and Møre Basin) it is dominated by mudstones with common layers of tuffaceous material and occasional interbedded sandstones; while to the south (e.g. in the Judd, Foinaven and southern Flett sub-basins) it is much sandier, and also contains coals and significantly less tuffaceous material (Watson *et al.* 2017). The Balder Fm. is typically ~18-60 m thick, and occurs across most of the FSB but is locally missing over the Erlend and Brendans Igneous Centres and the SE margin of the basin (Knox *et al.* 1997; Mudge 2015).

Thanetian-Ypresian Unconformities

A major incision surface (previously termed the Flett Unconformity) in the Judd Sub-basin has received substantial academic interest, being described by several authors (Fig. 3; Smallwood and Gill 2002; Shaw Champion *et al.* 2008; Hartley *et al.* 2011). This incision surface is recognized as an irregular, typically high-amplitude, unconformable seismic reflection, and forms an extensive NW-trending dendritic drainage system which has been mapped over an area of ~3000 km² in the Judd Sub-basin. There is some uncertainty regarding the age and magnitude of the uplift that resulted in incision of this drainage system, as well as the rates of both uplift and subsequent subsidence. Smallwood & Gill (2002) used the maximum valley depth

to estimate that the minimum uplift was 200 m, which occurred in sequence T45 times at a rate of 100-500 m Myr⁻¹, with the drainage system being incised into the top of the Flett Fm. and infilled by the Balder Fm. during subsequent subsidence (with estimated rates of 750-1100 m Myr⁻¹). Shaw Champion *et al.* (2008) used the maximum thicknesses of the Balder and Flett Formations to estimate a minimum uplift of 490 m (plus 60 m of isostatic uplift due to erosion) occurring within early sequence T40 (Flett Fm.). They calculated the minimum uplift rate at 220 m Myr⁻¹, and the following subsidence rate at 180-930 m Myr⁻¹. Hartley *et al.* (2011) modelled the profiles of individual channels and concluded that the area was uplifted in three steps of 200-400 m during sequence T38 (uppermost Lamba Fm.), early sequence T40 (Flett Fm.) and latest sequence T40 (Flett Fm.), with total uplift of ~900 m and an uplift rate of 500-3000 m Myr⁻¹. Both Shaw Champion *et al.* (2008) and Hartley *et al.* (2011) conclude that the drainage system was incised into the top of the Lamba Fm. and older units, with channel infill comprising Flett to Balder Fm. sedimentary rocks. Although their calculated rates of uplift and subsidence vary significantly, Smallwood and Gill (2002), Shaw Champion *et al.* (2008) and Hartley *et al.* (2011) agree that both were rapid, with the coupled cycle of uplift and subsidence occurring in less than 3 Myrs, and all suggest that the uplift was likely related to hot pulses within the Iceland Plume.

Previous workers have concluded that the observed uplift cannot be due to magmatic underplating as this would result in permanent rather than transient uplift, and thus attribute it to the transient passage of hot buoyant plume material beneath the lithosphere. Smallwood and Gill (2002) proposed that abnormally-hot mantle material became confined to the incipient NE Atlantic rift as it opened at ~55 Ma, resulting in the removal of thermal support and consequently leading to subsidence of the FSB. This hypothesis is supported by geochemical

analysis of compound lava flow sequences on the Faroe Islands undertaken by Millett *et al.* (2020), which indicates that mantle temperatures and melting were reduced at the sequence T40-T45 boundary. This reduction was linked to a regional volcanic hiatus, during which time rift-centered magmatism became dominant. In addition, Hardman *et al.* (2018b) used 3D seismic data to map paleocoastlines within sequence T50-60 above the Cambo and Westray Highs in the central FSB, and concluded that dynamic support from the Iceland Plume resulted in gradual subsidence ($\sim 330 \text{ m Myr}^{-1}$) during latest sequence T40-T45 ($\sim 55.8\text{-}55.3 \text{ Ma}$). This was followed by more rapid subsidence ($\sim 720\text{-}770 \text{ m Myr}^{-1}$) attributed to refocusing of the magma flow regime to the rift zone combined with cooling of the thermal anomaly.

Importantly, detailed biostratigraphical analysis of wells in the Judd Sub-basin undertaken by Jolley *et al.* (2021) reveals that the incision surface interpreted by Smallwood and Gill (2002), Shaw Champion *et al.* (2008) and Hartley *et al.* (2011) actually comprises two amalgamated unconformities: the Flett Unconformity (FU) at the boundary between sequences T40 and T45 (early Ypresian), and the Upper Thanetian Unconformity (UTU) between the Lamba and Flett Formations (sequences T38 and T40; Fig. 2). The UTU appears to have been the more temporally-extensive unconformity, resulting in a time gap of $\sim 0.5 \text{ Myrs}$, compared to the FU at $\sim 200 \text{ kyrs}$, with $\sim 1 \text{ Myrs}$ of subsidence and sedimentation occurring between them (Jolley *et al.*, 2021). Both unconformities have been identified in several wells across the FSB, from the extreme south to the northern part of the basin (Fig. 1 & 2).

A similar unconformity has also been identified in the Bressay area of the North Sea (Fig. 3; Underhill 2001; Stucky de Quay *et al.* 2017). The original seismic interpretation by Underhill (2001) concluded that this unconformity occurred at the top of sequence T45, with incision occurring into the top of the Dornoch Fm. More recent interpretation undertaken by Stucky de

Quay *et al.* (2017), however, using 3D seismic along with biostratigraphic and sedimentological data, indicates that the unconformity is actually at the base of sequence T40 and records incision into the Lista Fm. The upper part of the Lista Fm. in the North Sea is equivalent to the Lamba Fm in the FSB, indicating that the Bressay Unconformity was approximately coeval with the UTU, with the drainage system covering an area of approximately 100 km². Stucky de Quay *et al.* (2017) modelled channel profiles associated with this unconformity and concluded that the area was uplifted by at least 350 m, occurring in three separate steps at similar times to those identified by Hartley *et al.* (2011) in the Judd sub-basin.

Volcanic Succession

Volcanism in the FSB occurred as part of the NAIP, which can be subdivided into two main phases: a pre-rift phase, predating continental breakup, and a syn-rift phase, which occurred synchronously with breakup and marked the transition from rift to drift tectonics leading to the onset of seafloor spreading in the North Atlantic (Jolley and Bell 2002b; Chambers *et al.* 2005; Hansen *et al.* 2009; Walker *et al.* 2020).

Pre-breakup volcanism (Sequence T26-T40; Vaila Fm. to mid-Flett Fm.)

Within the FSB the earliest evidence for volcanic activity comprises tuffs and volcanoclastic material of Selandian age (sequences T26, T34-35; Vaila Fm.) found in cores and ditch cuttings (Jolley and Bell 2002b; Watson *et al.* 2017). Localized basaltic lava fields erupted during sequence T36 (early Lamba Fm.), preserved on the flank of Brendans Volcanic Centre (Jolley 2009; Mclean *et al.* 2017) and in the Foula Sub-basin, along with widespread deposition of the Kettla Tuff Member (Eidesgaard and Ziska 2013; Schofield *et al.* 2015; Watson *et al.* 2017).

Following a regional volcanic hiatus, widespread extrusive volcanism recommenced during Sequence T40 (Flett Fm., Jolley and Bell, 2002). Basaltic volcanic successions, comprising

lava flows, hyaloclastites and volcanoclastic facies, erupted across both margins of the NE North Atlantic from widespread fissures and shield volcanoes (e.g. Naylor et al., 1999; Jolley and Bell, 2002; Passey and Bell, 2007; Hansen et al., 2009; Passey and Jolley, 2009; Ritchie et al., 2011; Walker et al. 2020b).

Syn-breakup volcanism (latest sequence T40-T50; upper Flett Fm. to Balder Fm.)

During a volcanic hiatus at the end of sequence T40 (mid-Flett Fm.) a widespread unconformity developed (Jolley et al. 2021). Volcanism resumed in sequence T45 (coeval with deposition of the upper Flett Fm.), focused around the site of the proto-spreading axis. This syn-breakup succession was rapidly erupted during sequence T45 (Jolley 2009; Passey and Jolley 2009) but is largely absent from the FSB, with only localized lava fields recognized around the Corona Ridge, in the Judd Sub-basin and onshore in the Faroe Islands (Schofield and Jolley 2013).

In sequence T50 (Balder Fm.) volcanism was localized to the presumed site of seafloor spreading between East Greenland and the Faroe Islands. Flooding of the emerging spreading centre caused widespread phreatomagmatic eruptions, resulting in regional deposition of Balder Fm. tuffs (Roberts et al. 1984; Jolley and Bell 2002b; Jolley and Widdowson 2005; Watson et al. 2017).

Data and Methods

This study utilised a ~10,000 km² merged 3D seismic reflection survey (Northern Lights) in the northern Faroe-Shetland Basin, which comprises eight time-migrated 3D surveys acquired between 1999 and 2014, and reprocessed in 2016 by TGS (Table 1). Well data, including stratigraphic tops, partial wireline data and end-of-well reports, were available for all released

wells in the study area from the National Data Repository (NDR). Within the area of the seismic survey, wireline logs from four key wells were used to aid interpretation: 208/15-1A, 208/15-2, 209/06-1, and 209/12-1.

Seismic Interpretation

Horizons

Six main horizons were mapped across the study area: Top Balder Fm., Top and Base Basalt, the Flett and Upper Thanetian Unconformities and the Top Cretaceous. Seismic interpretation was undertaken using Schlumberger Petrel software, and horizons were mapped using seismic reflection characteristics (see Table 2) combined with stratigraphic tops in key wells where data quality allowed. The seismic data is typically of high quality, allowing for high confidence in horizon picking, except for areas underlying the volcanic succession and sill intrusions. This was not a significant issue, however, as this study focuses mainly on the FU and UTU outwith the volcanic cover, which are situated above intrusions. The UTU in particular is difficult to interpret in the vicinity of the Erlend Volcano due to the influence of the extrusive volcanic rocks, but this forms only a minor part of the study.

Spectral Decomposition

The Northern Lights seismic survey was used to produce an RGB frequency spectral decomposition of the Flett Unconformity incision surface using Geoteric software (Fig. 4). The process of spectral decomposition involves generating frequency bands from the seismic data and then assigning these frequencies to red, green and blue colour channels, which is useful to aid in the interpretation of subtle geomorphological features, e.g. fluvial channels and shorelines (Partyka *et al.* 1999). For this study, frequency bands of 21 Hz (red), 27 Hz (green) and 39 HZ

(blue) were used to create the spectral decomposition of the incision surface. This frequency range was chosen to give good coverage of the broad frequency spectrum of the seismic data, and to ensure optimal imaging of the varying thicknesses of the incised channel system.

Seismic Resolution

Vertical seismic resolution is the minimum thickness that a feature must have to be visible as a discrete seismic event; i.e. allowing two separate features to be distinguished from one another (Sheriff and Geldart 1982; Kearey and Brooks 1991). Subsurface features can produce a reflection at thicknesses less than this, with the minimum thickness required known as the limit of detectability (Brown 2011; Schofield *et al.* 2015; Eide *et al.* 2018). Both resolution and detectability are dependent on the seismic wavelength, which is calculated using the formula $\lambda = \frac{v}{f}$, where λ is the seismic wavelength (m), v is the interval velocity (m/s) and f is the dominant seismic frequency (Hz) (Widess 1973). Vertical seismic resolution is taken to be $\lambda/4$, while the limit of detectability is commonly assumed to be between $\lambda/8$ and $\lambda/30$, varying depending on factors such as seismic noise, the reflectivity of strata surrounding the feature of interest, and processing of the data (Widess 1973; Brown 2011; Schofield *et al.* 2015; Eide *et al.* 2018). At the depth of interest for this study, the dominant frequency of the seismic data is typically ~25 Hz and the average velocity from the wells is ~2.3 km/s, giving a seismic wavelength of ~92 m. In the region of investigation of the unconformity surface, therefore, vertical resolution is ~23 m, and the limit of detectability varies between ~3-11.5 m.

Wireline Logs

The four wells in the study area (208/15-1A, 208/15-2, 209/06-1 and 209/12-1) were all drilled between c. 25-40 years ago (1979, 1995, 1980 and 1985, respectively) and the intervals

of interest for this study (i.e. the mapped unconformity surfaces) are generally much shallower than the intended exploration targets of the wells. As a result, only partial wireline data is available for these intervals, with sonic, density and even caliper logs typically being missing, incomplete or of poor/inconsistent quality (Table 3). Caliper data is available only for 208/15-2 and reveals substantial caving over the interval of interest, which is linked to very low density values (and high correction values), and very low sonic log velocities (a common feature of washed out well sections). For the other wells (208/15-1A, 209/06-1, 209/12-1), caliper curves at the depth of interest are missing from the main log suite; however, caliper data from the deviation survey indicates that caving and poor borehole conditions were also an issue for these wells. The only log data available for all wells is gamma ray and partial deep resistivity (Table 3).

Gamma ray log responses over the focus intervals are clearly not normalized and display a wide variation for equivalent muddy or sandy layers (based on composite log lithologies) between wells. No new cuttings analyses was undertaken in this study, so in order to gain some insight regarding the sedimentary sequence in the zone of interest, a simplified gamma cut-off for “sand-prone” versus “mud-prone” has been applied to each well. The cut-offs were chosen based broadly on a ~25% shale volume (Vsh) value guided by the gamma ranges for each well (so that <25% Vsh was taken as “sand-prone” and vice versa), alongside reference to the reported cuttings-based lithologies. Additional simplified lithologies such as coal/lignite, tuffaceous rocks and carbonates were also included based on the composite log reports.

Seismic-Well Tie

To create an accurate seismic-well tie, robust density and sonic log data are required over the interval of interest. Such data is available only for 208/15-2; however, the main variations in both density and sonic logs over the focus interval are exclusively linked to major

caving horizons, leading to greater variations in both logs than is related to any lithological variations. The resulting synthetic seismic trace clearly delivers a result dominated by borehole conditions rather than lithology, and therefore cannot be compared reliably to the seismic data. It was therefore not possible to petrophysically tie the wells to the seismic data for the shallow intervals of interest in this area.

Using released VSP and checkshot data to tie the wells to the seismic data results in significant discrepancies between stratigraphic well tops in the different wells (e.g. The Top Balder Fm. within 209/6-1 apparently corresponds to a completely different seismic reflection than in 209/12-1). This indicates that the VSP and checkshot data for the wells within the study area are of variable and uncertain quality, possibly due to their ages (>25 yrs). Thus, while the wells can be approximately tied to the seismic (enough for broad interpretation of major sequence boundaries, e.g. Top Cretaceous), it is not accurate enough for highly detailed interpretation of intra-sequence boundaries. The incision surface forming the primary interest of this study is therefore interpreted based entirely on seismic character.

Results

Well Analysis

The well correlation in Fig. 5 shows intervals of the key wells between the late Paleocene (Vaila Fm., sequence T35 and Lamba Fm., sequence T36-38) and early Eocene (Balder Fm., sequence T50), with these sequences based on the available biostratigraphic data and released composite logs. Two unconformities are identified within the wells. The Upper Thanetian Unconformity (UTU) coincides with the top of the Lamba Fm., and is underlain by sequence T36-38 sedimentary rocks and overlain by uppermost sequence T40. The Flett Unconformity (FU) corresponds approximately to the boundary between the Upper and Lower

Flett Fm., being underlain by uppermost sequence T40 and overlain by mid-sequence T45 strata. These two unconformity surfaces are typically close together: within 208/15-1a and 209/12-1 they are separated by ~25 m of strata; this thickens to ~35 m in 209/6-1; and the surfaces are furthest apart in 208/15-2, where they are separated by ~75 m of strata.

Analysis of wireline data reveals that, at least in the vicinity of the wells, the drainage system responsible for formation of the FU and UTU incised into predominantly mud-dominated facies. Much of the late Paleocene-early Eocene sequence is dominated by mud-rich sedimentary facies, particularly the Vaila and Lamba Formations (Selandian-Thanetian; sequence T35-38) beneath the UTU, which comprise almost exclusively muddy sedimentary rocks (Fig. 5). The Lower Flett Fm. (latest Thanetian-Ypresian; sequence T40) between the FU and UTU is also commonly mud-rich, except in 208/15-2 where it contains numerous beds of sandy material between ~1348 m and ~1420 m depth, ranging in thickness from <1 m to ~12 m (>50% “sand-prone”); and in 209/6-1, where it contains a single ~4 m-thick sand-prone bed (~1516 m depth) and three beds (<1-5 m) of tuffaceous material (~1498-1515 m depth, based on composite log lithology descriptions). Above the FU, the Upper Flett Fm. (Ypresian; sequence T45) is dominated by mud-rich facies in 208/15-2 and 209/12-1, with thin sandy beds up to 2 m thick. In 209/6-1 sequence T45 occurs as a ~35 m-thick sand-prone unit, and in 208/15-1a it comprises a lower ~7 m thick sand-prone unit, and an upper ~28 m thick mud-dominated unit with some thin sandy beds and a ~2 m thick coal seam at ~1475 m. The Balder Fm. (sequence T50) has variable thickness and lithology: in 209/12-1 it comprises a ~40 m-thick tuffaceous unit (the Balder Tuff); in 209/6-1 and 208/15-1a the lower half of sequence T50 comprises a mixture of sands and muds (with a basal ~3 m coal seam at the base in 209/6-1), while the upper half is

almost entirely mud-rich; and in 208/15-2 it contains 3 sand-rich sequences ~10-35 m thick separated by mud-rich units.

Seismic Interpretation

Paleotopography and Stratigraphy

The Paleogene paleotopography of the study area, revealed by mapping the Flett Unconformity (i.e. the top of sequence T40; Fig. 1, 3 & 5) is dominated by the highs of the Erlend Volcano to the north and the North Shetland Platform (NSP) to the south and east of the study area, and the Flett sub-basin to the west and Møre Basin to the NE. The Erlend high comprises the edifice of the Erlend Volcano and younger onlapping fissure lava flows (Walker *et al.* 2021). The NSP has a seismically chaotic internal character and its crest is represented by a very high-amplitude positive reflection (Fig. 7). In several nearby well penetrations on the North Shetland Platform (1/04-1, 1/04-2 and 208/24-1a) and Margerita Spur (210/4-1a and 210/5-1) the pre-Cretaceous sequence includes mud-rich Upper Jurassic strata, Permian-Triassic and Devonian sandstones. Across much of the central and southern FSB the basement is Lewisian in age (~2.7 Ga; Holdsworth *et al.* 2019), with some occurrences of Dalradian and Moine basement, particularly on and around the Shetland Islands (Ritchie *et al.* 2011). The exact age and nature of the North Shetland Platform in the study area is unknown, however nearby basement penetrations (e.g. 209/9-1) indicate that the basement, which is granitic to gneissic in character, is probably Caledonian in age (~490 – 390 Ma) (Ritchie *et al.* 2011; APT and Chemostrat, 2021).

The basin fill of the Flett Sub-basin comprises Cretaceous and younger sedimentary rocks, typically expressed in seismic data by clear sub-parallel and sub-horizontal reflections which onlap the flank of the NSP at the eastern edge of the basin (Fig. 7). These sequences,

particularly the Cretaceous, contain numerous high-amplitude saucer-shaped reflections representing mafic sill intrusions. The Paleocene sequence (including sequence T40) thickens dramatically basinwards in the Flett sub-basin, from 200 ms TWT or less near the NSP to >1 s TWT in the vicinity of 208/15-1a, coinciding with deepening of the top of the Cretaceous (Fig. 8). The Flett Unconformity (i.e. top of sequence T40) gradually deepens in a basinward direction in both the Møre Basin and Flett sub-basin (Fig. 6).

Incision Surface

A key observation from the interpretation of the seismic data is the presence of a widespread, highly irregular and undulating surface in the eastern part of the study area, which is incised into the underlying strata resulting in cross-cutting and truncation of underlying reflections (Figs. 6 and 7). This incision surface is represented by a high-amplitude positive reflection, which is typically higher-amplitude at the base of the incisions and lower-amplitude on the intervening highs and is commonly overlain by a high-amplitude negative reflection. Within deeper incisions there is often a very low-amplitude “infill” between these two reflections (Fig. 8). Although it has not been possible to tie the four wells used in this study to the seismic data due to the incomplete and poor-quality nature of the wireline datasets (as discussed previously), this incision surface appears likely to correspond to the Flett Unconformity identified from biostratigraphic analysis. The UTU is often not visible on the seismic data, either due to having been removed by the overlying FU or due to the separation between the two unconformity surfaces being below the vertical seismic resolution, resulting in both surfaces being represented by a single seismic reflection (e.g. as in 208/15-1a and 209/12-1). The UTU can however be clearly separated from the FU in some areas, where it tends to be somewhat lower-amplitude, e.g. in the vicinity of 209/6-1 and 208/15-2 (Figs. 7 and 8). Both

unconformities are also easily interpreted along much of the flank of the North Shetland Platform (Fig. 7). The UTU is clearly observed to overlie the Erlend volcanic edifice (Fig. 9) and can be tentatively traced between the edifice and the overlying volcanic rocks at the southern edge of the Erlend Volcano.

When mapped out in three dimensions, the Flett Unconformity is revealed to form an extensive dendritic drainage system, ~30km wide by ~50 km long and covering ~980 km² of the NE FSB between the Erlend Volcano and North Shetland Platform (Figs. 3 and 5). The channels of the drainage system are observed as deeply-incised sinuous valleys, separated by intervening highs. Individual channels are up to ~30 km in length, 2 km wide and 100 ms TWT (~100 m) in depth. The main trunk stream of the drainage system (shown in dark blue on fig. 6b) extends westwards through the valley between the Erlend volcano and the NSP and can be traced for ~30 km before it enters the Flett Sub-basin to the SW of the Erlend High. The trunk stream is fed by numerous tributaries ranging in length from just 1-2 km to ~25 km, sourced mostly from the NSP to the south with several originating from the Erlend Volcano to the north. These tributaries are often nearly perpendicular to the trunk stream. The largest tributary systems incise into the crest of the NSP at their upstream ends (Fig. 7), but the majority of the small tributary streams originate on the flanks of the platform, typically incising into Lamba Fm. sediments and progressively older units approaching the high. On the Erlend high the drainage system appears to be significantly less well-developed and less extensive than on the flanks of the North Shetland Platform, with few well-developed channels observed. Some of these channels appear to incise into sedimentary units overlying the volcanics, while others clearly incise into the top of the basalt (Fig. 9).

In addition to the “main” drainage system feeding into the trunk stream, there are several smaller separate systems (Fig. 6). Two channels flow northwest from the NSP into the Flett Sub-basin south of 209/12-1, distinct from the trunk stream (shown in red on fig. 6b). A drainage system is observed close to the southern edge of the seismic survey, which flows southwards from the crest of the NSP and extends beyond the edge of data coverage for this study (shown in purple on fig. 6b). Three smaller channel systems are also observed flowing northwards towards the Møre Basin: one from the NSP, one on the flank of the Erlend edifice, and a third located between the two (shown in light blue on fig. 6b).

There appears to have been some interaction between the drainage system and folds above intrusions (Fig. 10). On the seismic profile presented in Fig. 10, channels are observed to occur preferentially at the margins of forced folds above sills, with the fold crests largely remaining channel-free. In 3D, channels can be seen to be deflected around forced folds (shown in orange on fig. 6b), although in rare cases the folds may be incised. Similar interactions between forced-folds and turbidites in deeper settings of the Flett and Muckle subbasins have also been reported by Egbeni *et al.* (2014).

The character of the FU changes significantly across the study area, which corresponds broadly to the depth of the FU horizon. In the central region, around and between the Erlend Volcano and the North Shetland Platform (where the surface is shallower), the unconformity comprises numerous deeply-incised channels, resulting in the clear dendritic drainage system shown in Fig. 6. To the north (towards the Erlend Sub-basin) and west (into the Flett sub-basin) however, there are no clear incisions, resulting in a much smoother horizon that gradually deepens basinward.

Spectral Decomposition

Spectral decomposition analysis of the Flett Unconformity surface (Figs. 3 and 10) confirms the change in character of the FU. The NSP and Erlend Volcano are both extremely bright (high-amplitude), indicating their “hard-rock” nature (being primarily composed granitic to gneissic basement and basalt, respectively), and between them the drainage system is revealed as numerous channels of varying brightness incising into dark (low-amplitude) background sedimentary rocks. The channels are typically brightest just downstream of the crest of the NSP (Fig. 4). To the north the FU is generally dull with few clear features, while to the west the surface has varying brightness but few channel structures. Interesting features revealed by the spectral decomposition include a number of distinct curvilinear changes in brightness and colour (Fig. 4). Three are located to the west of Erlend, between 209/6-1 and 208/15-1a, which trend approximately N-S and appear to align with sedimentary ridge structures overlying the FU surface (Fig. 11). Another three are located to the east of Erlend, between the volcanic edifice and the NSP, which trend NW-SE and appear to correspond to onlapping of overlying units onto the FU surface rather than ridge-like structures (Fig. 12).

Discussion

Seismic analysis of Thanetian-Ypresian strata within the northern FSB has revealed two significant partially-merged incision surfaces forming a spectacular dendritic drainage system (Figs. 3 and 5). These drainage networks were formed during the development of regional Flett Unconformity and Upper Thanetian Unconformity (Jolley *et al.* 2021), and can therefore be correlated with similar systems previously identified within the Judd Sub-basin (Smallwood and Gill 2002; Shaw Champion *et al.* 2008; Hartley *et al.* 2011).

Distribution of Incised Channels

While the composite unconformity surface can be interpreted across the entire study area, the two unconformities are observed separately in only a few spatially-restricted areas in the Flett Sub-basin. Elsewhere the Upper Thanetian Unconformity surface appears to be truncated by the overlying Flett Unconformity, which may be a result of much of the UTU being removed by erosion associated with the FU, with only small areas being preserved where the erosion was less deep. An alternative possibility is that the FU exploited incised channels formed during the UTU rather than significantly eroding them, so that parts of the mapped drainage system can be considered to belong to both unconformities. It is plausible that both mechanisms may have occurred, with the largest channels (e.g. the trunk stream shown in blue on fig. 6) being formed during the UTU and exploited by the FU, while in other areas the UTU was eroded away.

Within the study area, the incised channels are clearly concentrated in the region between the Erlend Volcano and the NSP, with tributaries extending up on top of those highs. Further north, into the Erlend sub-basin, incised channels are not evident even on the crest of the NSP, and while some channels are visible further south along the NSP, they are far less frequent and interconnected. This suggests that proximity to the Erlend Volcano exerts a strong control on the formation of the incision surface, possibly due to localised uplift around the edifice. The volcano is underlain by a large laccolithic plumbing system and sill complex (Walker *et al.* 2021), and it is known that the area beneath the edifice was uplifted during latest Cretaceous-Paleocene times, based on biostratigraphy and missing Early Paleocene sedimentary strata in 209/3-1 (Jolley and Bell 2002a). The area surrounding the volcanic edifice, is also heavily

intruded by sills of the Faroe-Shetland Sill Complex, which are overlain by forced fold structures showing that they have also contributed to localised uplift (Mark et al. 2018). The Judd and Corona regions are also heavily intruded by sills (Hardman et al. 2018a), so it is possible that, as well as proximity to the basin margin, uplift due to significant volumes of intrusions (in addition to the regional uplift) was necessary for formation of major drainage systems. This could explain why the Bressay drainage system is smaller and more localised than those in the FSB (~100 km² vs ~1000+ km²), as there are no intrusions in this region.

On a more regional scale drainage networks also appear to be concentrated in specific parts of the FSB. Although the FU and UTU are recorded in wells across the FSB, as well as in the Rockall Basin and North Sea (Fig. 1) (Jolley et al. 2021), clear incised drainage systems have been identified only within the Judd Sub-basin (Smallwood and Gill 2002; Shaw Champion et al. 2008; Hartley et al. 2011; Hardman et al. 2018b; Jolley et al. 2021), on the Corona High (Hardman et al. 2018a) and in the northern Flett Sub-basin (this study), along with a more localised incision surface on the East Shetland Platform - Bressay area of the North Sea (Stucky de Quay et al. 2017) (Fig. 3). These drainage systems are located on or close to the basin margin or intra-basinal highs. It therefore seems likely that channels were primarily incised on existing structural highs, particularly the shoulders of the basins, which were uplifted above sea level and therefore non-marine, whereas deeper areas (e.g. the continental shelf) were locations of sedimentary bypass or nondeposition without active incision. Although no incision surfaces have currently been mapped along the West Shetland Platform or Rona High between the Judd and Flett sub-basins, or beneath the basalt cover to the west (Fig. 3), it is entirely possible that they occur there but have not yet been identified.

Relationship to Volcanism

The estimated ages of the unconformities have important implications for the dating of volcanism in the study area. The volcanic succession comprises two separate basaltic sequences: the older sequence forms the Erlend volcanic edifice, and the younger sequence is made up of subaerial lava flows onlapping the edifice (Walker *et al.* 2021). Both sequences have previously been assigned to sequence T40 based on biostratigraphic evidence (Jolley and Bell 2002a), but due to significant challenges in radiometric dating of basaltic rocks (e.g. Wilkinson *et al.* 2016; Walker *et al.* 2020; Jolley *et al.* 2021), there are no available isotopic ages for the Erlend basaltic sequences. The interpretation of the seismic data by this study indicates that both the FU (top sequence T40) and UTU (top sequence T38) overlie and incise into the lavas. This strongly suggests that at least some of the volcanic deposits were erupted prior to the UTU and are part of the Lamba Fm. or older stratigraphic units. We note that it appears that the UTU may occur between the Erlend edifice and the younger onlapping lavas (Fig. 9), although it is difficult to be certain as the high seismic amplitudes of the lava flows make the UTU difficult to interpret. If this is the case, it indicates that the Erlend edifice was formed prior to the development of the UTU, while the onlapping lava sequence was erupted between the UTU and FU (i.e. during sequence T40) and can thus be reliably correlated with the widespread sequence T40 volcanism across the FSB. It is possible that the Erlend Volcano is a similar age to Brendan's Dome, a nearby igneous complex that has proven sequence T36 (latest Selandian-early Thanetian) lava sequences, based on biostratigraphic analysis of well data (Jolley 2009; Mclean *et al.* 2017). If so Erlend forms just the fourth example of sequence T36 extrusives in the FSB (the previous three being Brendan's Dome (219/21-1), 208/21-1 in the Foula Sub-basin (Schofield *et al.* 2015), and Anne-Marie (6004/8a-1) in the southern FSB (Jolley *et al.* 2021)). Given the relative ages of the

edifice and the UTU, it is likely that Erlend was no longer actively uplifting at the time of incision, but rather formed an existing high. This explains the high angles (often approaching 90°) between the trunk stream of the drainage system and its tributaries, with the tributaries flowing perpendicularly down the flank of the NSP, being diverted by the edifice and effectively funnelled westwards along the valley between the two highs.

The drainage system was also clearly influenced by sill intrusions beyond the volcanic edifice, with several instances of channels being diverted around forced fold structures. Above the sills, thickness changes observed in the strata directly overlying the top of the Cretaceous indicate that the folds were growing (and therefore that the sills were being intruded) during early Paleocene times (Fig. 10), up to 5 Myrs before formation of the incision surfaces. The fact that the drainage systems were deflected, even though the folds were buried and long since inactive, shows that forced fold structures can form positive features at the surface and influence sedimentation for millions of years after their formation.

Post-Incision Basin Evolution (Paleoshorelines)

The curvilinear changes in amplitude visible on the spectral decomposition (Fig. 4) are likely to represent preserved coastlines, based on their geometries and parallel nature (Jackson *et al.* 2010; Hardman *et al.* 2018b; Berton *et al.* 2021). The coastlines to the east and west of Erlend have very different cross-sectional morphologies, which may be related to the slope of the paleosurface at the time of flooding. To the west the paleosurface appears to have been fairly flat, allowing for the build-up of ridges of sediment along the coast (Fig. 11); while to the east the paleosurface was dipping to the NE, which prohibited the formation of such ridges so that the coastlines were preserved as simple onlapping structures (Fig. 12). Although it is

difficult to determine the precise age of these coastlines due to lack of well control, they appear to be very similar in age, occurring within sequence T45 just above the Flett Unconformity surface (and thus may be equivalent to the upper Colsay Mb. of the Flett Fm.; Hardman *et al.*, 2018a). The eastern coastlines show progressive onlapping onto the FU, indicating movement of the coastline inland and flooding of the uplifted high. Such relationships are not clear for the ridge-like structures to the west, but given the apparent similarity in age between the two sets of coastlines it is reasonable to assume that they also record progressive flooding associated with marine transgression.

Comparison with Previous Studies

The findings of this study are largely in agreement with previous studies on the FU and UTU. There were clearly two phases of uplift resulting in incision and formation of the two unconformities, separated by a period of subsidence allowing deposition of sequence T40 sediments, in agreement with the conclusions of Jolley *et al.* (2021). The coastlines identified to the east and west of the Erlend incision surface indicate that subsidence began during sequence T45 shortly after formation of the FU, which supports the findings of Hardman *et al.* (2018). This study also broadly agrees with the findings of Smallwood and Gill (2002), Shaw Champion *et al.* (2008) and Hartley *et al.* (2011) regarding the timing of incision, with the caveat that those studies did not identify the two distinct unconformities.

Many of the previous studies attributed the uplift resulting in the FU and UTU to the Iceland Plume, based on its transient nature. While the results of this study show that the uplift was indeed short-lived and immediately followed by subsidence, which may support the plume conclusion of Smallwood and Gill (2002), Shaw Champion *et al.* (2008), Hartley *et al.* (2011) and

Hardman *et al.* (2018), there is not enough evidence to definitively attribute the uplift to the plume or to other (e.g. tectonic) factors.

Impact on Hydrocarbon Prospectivity

Much of the Flett and Upper Thanetian drainage systems are incised into older Paleocene (mostly Lamba Fm.) sedimentary strata, incising into progressively older units towards the basin margin. In the northern FSB the majority of the Upper Cretaceous to Lamba Fm. are known from well data (e.g. 208/15-1a, 208/15-2, 209/6-1, 209-12-1, 219/21-1) to be largely mud-dominated, and thus eroded sediments are likely to have limited reservoir potential. However, it is clear from the seismic data that the drainage system is also incised into the top of the North Shetland Platform at the eastern edge of the FSB (Fig. 7). Given that the NSP is likely to comprise granitic to gneissic crystalline basement (based on comparison with nearby wells and other structural highs in the FSB), erosion of the platform would have resulted in the formation of potentially clean high quality siliciclastic sediments.

The potential distribution of reservoir sands related to the drainage system is largely conjectural, although it is possible to highlight several areas where they are more likely. Spectral decomposition on the FU surface reveals exceptionally bright amplitudes within several of the channels just downstream of the crest of the NSP (Fig. 4), which may be indicative of high sand content. While it is possible that fluvial sands may remain within the incised channels, sands are also likely to have been deposited in more basinal areas. Given that sediment reworking is typically key to producing clean reservoir sands, and that significant reworking commonly takes place within coastal (especially beach) environments, the coast-line deposits highlighted by the spectral decomposition, and surrounding areas, may have the highest potential for clean

sandstones. Evidence for this can be seen in the key wells: e.g. in 208/15-2 sequence T40 is sand-prone, with the cleanest sandstones occurring ~10 m above the UTU; and in 209/6-1, sequence T45 overlying the FU also appears to be sand rich. In addition, the Tobermory (214/4-1) and Bunnehaven (214/9-1) wells ~70 km E of the Erlend Volcano both contain Flett Formation (sequence T40-45) sandstones, and while the origin of these sands cannot currently be proven, it cannot be ruled out that they are associated with the drainage system mapped in this study.

In addition to the impact of transport and reworking, another important factor for potential reservoir quality in this region is that of volcanoclastic input into the depositional system. Mafic minerals within basaltic volcanic and volcanoclastic rocks are susceptible to weathering, breaking down into pore-clogging clay minerals and zeolite (Ólavsdóttir and Ziska 2009; Ólavsdóttir *et al.* 2015; Sætre *et al.* 2018). When volcanoclastic sediments are introduced into a clastic sedimentary system they can have a significant impact on the reservoir properties of sandstones, the extent of which is largely dependent on the relative amounts of clastic and volcanoclastic material. A large volcanoclastic input will typically result in a greater reduction of both porosity and permeability than a smaller amount (Larsen *et al.* 2018). However, small amounts of volcanoclastic sediments can lead to the early formation of chlorite rims around quartz grains, which has been shown to inhibit the formation of later quartz cementation, preserving porosity and permeability and leading to higher reservoir quality (Larsen *et al.* 2018; Sætre *et al.* 2018). Erosion of the Erlend volcanic sequences is clearly shown by the incision of channels into the top-basalt surface, indicating at least some volcanoclastic input to the drainage system. It is not clear how much of an impact this may have had, but of the key wells, only 209/6-1 (which is closest to the volcano) contains volcanoclastics (~5 m) within sequence T40,

and there are none within sequence T45. 209/12-1 contains a ~40 m-thick Balder Fm. tuffaceous unit, but this occurs well above the unconformity surfaces and therefore did not impact the drainage system. It is possible, therefore, that the amount of volcanoclastic material may have been small enough to have a positive impact on reservoir quality. The poor quality of archive well data precludes high confidence in the appraisal of volcanoclastics in the area; however, it is clear that volcanoclastics locally form a component of the drainage system and should be appraised further in future.

Conclusions

This paper presents detailed seismic mapping of a newly-identified incision surface in the northern Faroe-Shetland Basin. Combining the seismic interpretation with analysis of available well data has enabled important insights into surface movements of the FSB, the evolution of Paleocene-Eocene drainage systems and the impact on hydrocarbon prospectivity. The incision surface takes the form of an extensive dendritic drainage system between the Erlend Volcano and the North Shetland Platform, which comprises two partially-merged unconformities: the Upper Thanetian Unconformity spanning the sequence T38-T40 boundary (Lamba to Flett Fm. boundary) and the Flett Unconformity at the sequence T40-T45 boundary (intra Flett Fm.). The ages of the unconformities have important implications for volcanism in the area, showing that at least part of the Erlend Volcano may have formed prior to the UTU, and thus was active during Lamba Fm. times, adding to the small number of currently identified T36 volcanic sequences in the FSB (Jolley et al., 2021).

The UTU represents the earlier of the two mapped unconformities formed during a prolonged period of uplift, which was partially infilled during a phase of minor subsidence during

sequence T40. Renewed uplift at the sequence T40-T45 boundary resulted in formation of the FU and partial erosion of the UTU incision surface. In most areas the FU appears to have removed the majority of T40 sediments, which are locally preserved as seismically-resolvable channel fills within the UTU drainage system. In addition to the broad-scale channel features associated with regional uplift, clear evidence is presented for small scale uplift features associated with forced-folding above sill intrusions beneath the channel system. Although the sills were emplaced prior to the regional uplift, deflection of the drainage system shows that the forced folds formed positive features at the paleosurface and influenced sedimentation routes long after the folds had stopped growing.

Several curvilinear features occur close to the basinward limits of the mapped incision surface to the east and west of the Erlend edifice, which are interpreted as a series of preserved paleoshorelines. To the west, the paleosurface was relatively flat and the coastlines are represented by elongate sedimentary constructional ridges interpreted as beach deposits; while to the east the paleosurface was dipping and the coastlines are preserved as onlapping features. In both cases, the features record progressive backstepping of the shoreline associated with transgression during post-FU sequence T45 subsidence.

The drainage system described in this paper has key implications for hydrocarbon prospectivity in the northern FSB. Incision into the granitic to gneissic North Shetland Platform may have acted as an important source for siliciclastic sediments which, combined with downstream transportation and reworking have the potential to form high-quality clean reservoir sandstones. Although some of these sands may have been deposited within the channels themselves, they are most likely to have been deposited in the Flett Sub-basin both as shoreline deposits and further out into the basin. Understanding the sediment pathways and

probable locations for reservoir presence is of great importance to future exploration efforts in the region.

Acknowledgments

Funding from the U.K. Natural Environment Research Council (NERC) (Oil and Gas Centre for Doctoral training) and the British Geological Survey for Faye Walker's PhD is gratefully acknowledged. SP is partly supported by the Research Council of Norway through its Centres of Excellence funding scheme (project 223272 CEED). TGS (www.tgs.com) is thanked for providing access to the Northern Lights seismic data. Seismic interpretation was undertaken using Schlumberger Petrel software and IHS Kingdom Suite. Spectral Decomposition was undertaken using FFA Geoteric Software.

References

- APT and Chemostrat, 2021, Faroe-Shetland Basin Basement Characterization and Thermal Calibration Database & Report, (<https://data-ogauthority.opendata.arcgis.com/documents/OGAUTHORITY::apt-geochemical-evaluation-of-oil-provenance-quality-wos/about>)
- Berton, F., Vesely, F.F., Guedes, C.F.C., Souza, M.C. and Angulo, R.J. 2021. Subsurface geomorphology of wave-dominated nearshore deposits: Contrasting styles of reservoir heterogeneity in response to shoreline trajectory. *Marine and Petroleum Geology*, **124**, 104821, <https://doi.org/10.1016/j.marpetgeo.2020.104821>.
- Boldreel, L. and Andersen, M.S. 1993. Late Paleocene to Miocene compression in the Faeroe–Rockall area. *Petroleum Geology of Northwest Europe: Proceedings of the 4th Conference*, 1025–1034, <https://doi.org/10.1144/0041025>.
- Brown, A.R. 2011. *Interpretation of Three-Dimensional Seismic Data*.
- Chambers, L.M., Pringle, M.S. and Parrish, R.R. 2005. Rapid formation of the Small Isles Tertiary centre constrained by precise $^{40}\text{Ar}/^{39}\text{Ar}$ and U-Pb ages. *Lithos*, **79**, 367–384, <https://doi.org/10.1016/j.lithos.2004.09.008>.
- Clift, P. 1999. The thermal impact of Paleocene magmatic underplating in the Faeroe-Shetland-Rockall region. In: Fleet, A. J. and Boldy, S. A. R. (eds) *Petroleum Geology of Northwest Europe: Proceedings of the 5th Conference on the Petroleum Geology of Northwest Europe*. 585–594., <https://doi.org/10.1144/0050585>.

- Clift, P. and Turner, J. 1998. Paleogene igneous underplating and subsidence anomalies in the Rockall-Faeroe-Shetland area. *Marine and Petroleum Geology*, **15**, 223–243, [https://doi.org/10.1016/S0264-8172\(97\)00056-1](https://doi.org/10.1016/S0264-8172(97)00056-1).
- Conway-Jones, B. and White, N. 2020. Transient Buried Landscapes as Manifestations of Icelandic Plume Activity. In: *EGU General Assembly 2020*. EGU2020-551., <https://doi.org/https://doi.org/10.5194/egusphere-egu2020-551>.
- Coward, M.P., Dewey, J.F., Hempton, M. and Holroyd, J. 2003. Tectonic Evolution. In: Evans, D., Graham, C., Armour, A. and Bathurst, P. (eds) *The Millennium Atlas: Petroleum Geology of the Central and Northern North Sea*. 17–33.
- Doré, A.G., Lundin, E.R., Fichler, C. and Olesen, O. 1997. Patterns of basement structure and reactivation along the NE Atlantic margin. *Journal of the Geological Society, London*, **154**, 85–92, <https://doi.org/10.1144/gsjgs.154.1.0085>.
- Doré, A.G., Lundin, E.R., Jensen, L.N., Birkeland, Ø., Eliassen, P.E. and Fichler, C. 1999. Principal tectonic events in the evolution of the northwest European Atlantic margin. In: Fleet, A. J. and Boldy, S. A. R. (eds) *Petroleum Geology of Northwest Europe: Proceedings of the 5th Conference*. 41–61., <https://doi.org/10.1144/0050041>.
- Ebdon, C.C., Granger, P.J., Johnson, H. and Evans, A.M. 1995. Early Tertiary evolution and sequence stratigraphy of the Faeroe- Shetland Basin: implications for hydrocarbon prospectivity. In: Scrutton, R. A., Stoker, M. S., Shimmiel, G. B. and Tudhope, A. W. (eds) *The Tectonics, Sedimentology and Palaeoceanography of the North Atlantic Region*. 51–69.
- Egbeni, S., McClay, K., Jian-kui Fu, J. and Bruce, D. 2014. Influence of igneous sills on Paleocene turbidite deposition in the Faroe–Shetland Basin: a case study in Flett and Muckle sub-basin and its implication for hydrocarbon exploration. In: Cannon, S. J. C. and Ellis, D. (eds) *Hydrocarbon Exploration to Exploitation West of Shetlands*. 33–57.
- Eide, C.H., Schofield, N., Lecomte, I., Buckley, S.J. and Howell, J.A. 2018. Seismic interpretation of sill complexes in sedimentary basins: Implications for the sub-sill imaging problem. *Journal of the Geological Society*, **175**, 193–209, <https://doi.org/10.1144/jgs2017-096>.
- Eidesgaard, Ó.R. and Ziska, H. 2013. The Kettla Member An overview from the Faroe-Shetland Basin. In: *Faroe Islands Exploration Conference: Proceedings of 4th Conference*. 26–44.
- Ellis, D. and Stoker, M.S. 2014. The Faroe–Shetland Basin: a regional perspective from the Paleocene to the present day and its relationship to the opening of the North Atlantic Ocean. In: Cannon, S. J. C. and Ellis, D. (eds) *Hydrocarbon Exploration to Exploitation West of Shetlands*. 11–31.
- Hansen, J., Jerram, D.A., McCaffrey, K. and Passey, S.R. 2009. The onset of the North Atlantic Igneous Province in a rifting perspective. *Geological Magazine*, **146**, 309–325, <https://doi.org/10.1017/S0016756809006347>.
- Haq, B.U. and Al-Qahtani, A.M. 2005. Phanerozoic cycles of sea-level change on the Arabian platform. *GeoArabia*, **10**, 127–160.
- Hardman, J., Schofield, N., Jolley, D.W., Hartley, A., Holford, S. and Watson, D. 2018a. Controls

- on the distribution of volcanism and intra-basaltic sediments in the Cambo – Rosebank region , West of Shetland. *Petroleum Geoscience*, **25**, 71–89.
- Hardman, J., Schofield, N., et al. 2018b. Prolonged dynamic support from the Icelandic plume of the NE Atlantic margin. *Journal of the Geological Society*, jgs2017-088, <https://doi.org/https://doi.org/10.1144/jgs2017-088>.
- Hartley, R., Roberts, G.G., White, N. and Richardson, C. 2011. Transient convective uplift of an ancient buried landscape. *Nature Geoscience*, **4**, 562–565, <https://doi.org/10.1038/ngeo1191>.
- Haszeldine, R.S., Ritchie, J.D. and Hitchen, K. 1987. Seismic and well evidence for the early development of the Faeroe-Shetland Basin. *Scottish Journal of Geology*, **23**, 283–300.
- Holdsworth, R.E., Morton, A., Frei, D., Gerdes, A., Strachan, R.A., Dempsey, E., Warren, C. and Whitham, A., 2019. The nature and significance of the Faeroe-Shetland Terrane: linking Archaean basement blocks across the North Atlantic. *Precambrian Research*, **321**, 154-171.
- Jackson, C.A.-L., Grunhagen, H., Howell, J.A., Larsen, A.L., Andersson, A., Boen, F. and Groth, A. 2010. 3D seismic imaging of lower delta-plain beach ridges: lower Brent Group, northern North Sea. *Journal of the Geological Society, London*, **167**, 1225–1236, <https://doi.org/10.1144/0016-76492010-053.3D>.
- Jolley, D.W. 2009. Palynofloral evidence for the onset and cessation of eruption of the Faroe Islands lava field. In: *Faroe Islands Exploration Conference: Proceedings of the 2nd Conference*. 156–173.
- Jolley, D.W. and Bell, B.R. 2002a. Genesis and age of the Erlend Volcano, NE Atlantic Margin. In: Jolley, D. W. and Bell, B. R. (eds) *The North Atlantic Igneous Province: Stratigraphy, Tectonic, Volcanic and Magmatic Processes*. 95–110., <https://doi.org/10.1144/GSL.SP.2002.197.01.05>.
- Jolley, D.W. and Bell, B.R. 2002b. The evolution of the North Atlantic Igneous Province and the opening of the NE Atlantic rift. In: Jolley, D. W. and Bell, B. R. (eds) *The North Atlantic Igneous Province: Stratigraphy, Tectonic, Volcanic and Magmatic Processes*. 1–13., <https://doi.org/10.1144/GSL.SP.2002.197.01.01>.
- Jolley, D.W. and Morton, A.C. 2007. Understanding basin sedimentary provenance: Evidence from allied phytogeographic and heavy mineral analysis of the Palaeocene of the NE Atlantic. *Journal of the Geological Society*, **164**, 553–563, <https://doi.org/10.1144/0016-76492005-187>.
- Jolley, D.W. and Widdowson, M. 2005. Did Paleogene North Atlantic rift-related eruptions drive early Eocene climate cooling? *Lithos*, **79**, 355–366, <https://doi.org/10.1016/j.lithos.2004.09.007>.
- Jolley, D.W., Millett, J.M., Schofield, N., Broadley, L. and Hole, M.J. 2021. Stratigraphy of volcanic rock successions of the North Atlantic rifted margin : the offshore record of the Faeroe – Shetland and Rockall basins. *Earth and Environmental Science Transactions of the Royal Society of Edinburgh*, 1–28, <https://doi.org/10.1017/S1755691021000037>.
- Kearey, P. and Brooks, M. 1991. *An Introduction to Geophysical Exploration*, Second.
- Kimbell, G.S., Stewart, M., et al. 2017. Controls on the location of compressional deformation

- on the NW European margin. *Geological Society, London, Special Publications*, **447**, 249–278, <https://doi.org/10.1144/sp447.3>.
- Knox, R.W.O., Holloway, S., Kirby, G.A. and Baily, H.E. 1997. *Stratigraphic Nomenclature of the UK North West Margin: 2. Early Paleogene Lithostratigraphy and Sequence Stratigraphy*.
- Lamers, E. and Carmichael, S. 1999. The Paleocene deepwater sandstone play West of Shetland. *Petroleum Geology of Northwest Europe: Proceedings of the 5th Conference on the Petroleum Geology of Northwest Europe*, **1**, 645–660, <https://doi.org/10.1144/0050645>.
- Larsen, M., Bell, B., Guarnieri, P., Vosgerau, H. and Weibel, R. 2018. Exploration challenges along the North Atlantic volcanic margins: The intra-volcanic sandstone play in subsurface and outcrop. *Petroleum Geology Conference Proceedings*, **8**, 231–245, <https://doi.org/10.1144/PGC8.13>.
- McLean, C., Schofield, N., Brown, D.J., Jolley, D.W. and Reid, A. 2017. 3D seismic imaging of the shallow plumbing system beneath the Ben Nevis Monogenetic Volcanic Field: Faroe–Shetland Basin. *Journal of the Geological Society*, <https://doi.org/10.1144/jgs2016-118>.
- Millett, J.M., Hole, M.J., Jolley, D.W., Passey, S.R. and Rossetti, L. 2020. Transient mantle cooling linked to regional volcanic shut-down and early rifting in the North Atlantic Igneous Province. *Bulletin of Volcanology*, **82**, <https://doi.org/10.1007/s00445-020-01401-8>.
- Morton, A.C., Douglas Boyd, J. and Ewen, D. 2002. Evolution of Paleocene sediment dispersal systems in the Foinaven sub-basin, west of Shetland. *Geological Society Special Publication*, **197**, 69–93, <https://doi.org/10.1144/GSL.SP.2002.197.01.04>.
- Mudge, D.C. 2015. Regional controls on Lower Tertiary sandstone distribution in the North Sea and NE Atlantic margin basins. *Tertiary Deep-Marine Reservoirs of the North Sea Reservoirs of the North Sea*, 403, <https://doi.org/10.1144/SP403.5>.
- Mudge, D.C. and Bujak, J. 2001. Biostratigraphic evidence for evolving palaeoenvironments in the Lower Paleogene of the Faeroe-Shetland Basin. *Marine and Petroleum Geology*, **18**, 577–590, [https://doi.org/10.1016/S0264-8172\(00\)00074-X](https://doi.org/10.1016/S0264-8172(00)00074-X).
- Naylor, P.H., Bell, B.R., Jolley, D.W., Durnall, P. and Fredsted, R. 1999. Palaeogene magmatism in the Faeroe-Shetland Basin: influences on uplift history and sedimentation. *Petroleum Geology of Northwest Europe: Proceedings of the 5th Conference on the Petroleum Geology of Northwest Europe*, **1**, 545–558, <https://doi.org/10.1144/0050545>.
- Ólavsdóttir, J. and Ziska, H. 2009. Reservoir quality assessment of the volcanoclastic post-basalt sediments in the Faroese area of the Faeroe-Shetland Basin. *Most*, 227–240.
- Ólavsdóttir, J., Andersen, M.S. and Boldreel, L.O. 2015. Reservoir quality of intrabasalt volcanoclastic units onshore Faroe Islands, North Atlantic igneous province, Northeast Atlantic. *AAPG Bulletin*, **99**, 467–497, <https://doi.org/10.1306/08061412084>.
- Parnell-Turner, R., White, N., Henstock, T., Murton, B., Maclennan, J. and Jones, S.M. 2014. A continuous 55-million-year record of transient mantle plume activity beneath Iceland. *Nature Geoscience*, **7**, 914–919, <https://doi.org/10.1038/ngeo2281>.
- Partyka, G., Gridley, J. and Lopez, J. 1999. Interpretational applications of spectral

decomposition in reservoir characterization. *The Leading Edge*, **18**, 353–360, <https://doi.org/10.1190/1.1438295>.

Passey, S.R. and Bell, B.R. 2007. Morphologies and emplacement mechanisms of the lava flows of the Faroe Islands Basalt Group, Faroe Islands, NE Atlantic Ocean. *Bulletin of Volcanology*, **70**, 139–156, <https://doi.org/10.1007/s00445-007-0125-6>.

Passey, S.R. and Jolley, D.W. 2009. A revised lithostratigraphic nomenclature for the Palaeogene Faroe Islands Basalt Group, NE Atlantic Ocean. *Earth and Environmental Science Transactions of the Royal Society of Edinburgh*, **99**, 127–158, <https://doi.org/10.1017/S1755691009008044>.

Posamentier, H.W. and Vail, P.R. 1988. Eustatic controls on clastic deposition II - sequence and systems tract models. *Sea-Level Changes—An Integrated Approach, SEPM Special Publication*, **42**, 125–154, <https://doi.org/10.2110/pec.88.01.0125>.

Praeg, D., Stoker, M.S., Shannon, P.M., Ceramicola, S., Hjelstuen, B.O., Laberg, J.S. and Mathiesen, A. 2005. Episodic Cenozoic tectonism and the development of the NW European 'passive' continental margin. *Marine and Petroleum Geology*, **22**, 1007–1030, <https://doi.org/10.1016/j.marpetgeo.2005.03.014>.

Ritchie, J.D., Johnson, H., Quinn, M.F. and Gatliff, R.W. 2008. The effects of Cenozoic compression within the Faroe-Shetland Basin and adjacent areas. In: Johnson, H., Doré, A. G., Gatliff, R. W., Holdsworth, R., Lundin, E. R. and Ritchie, J. D. (eds) *The Nature and Origin of Compression in Passive Margins*. 121–136., <https://doi.org/10.1144/SP306.5>.

Ritchie, J.D., Ziska, H., Johnson, H. and Evans, D. (eds). 2011. *Geology of the Faroe-Shetland Basin and Adjacent Areas*.

Roberts, D.G. 1989. Basin inversion in and around the British Isles. In: Cooper, M. A. and Williams, G. D. (eds) *Inversion Tectonics*. 131–150.

Roberts, D.G., Morton, A.C. and Backman, J. 1984. Late Palaeocene-Eocene Volcanic Events in the Northern North Atlantic Ocean. In: Roberts, D. G. and Schnitker, D. (eds) *Initial Reports of the Deep Sea Drilling Project*. 913–923.

Roberts, D.G., Thompson, M., Mitchener, B., Hossack, J., Carmichael, S. and Bjørnseth, H. 1999. Palaeozoic to Tertiary rift and basin dynamics : mid-Norway to the Bay of Biscay – a new context for hydrocarbon prospectivity in the deep water frontier Palaeozoic to Tertiary rift and basin dynamics : mid-Norway to the Bay of Biscay - a new context for . *Petroleum Geology Conference Series*, **5**, 7–40, <https://doi.org/10.1144/0050007>.

Rudge, J.F., Shaw Champion, M.E., White, N., McKenzie, D. and Lovell, B. 2008. A plume model of transient diachronous uplift at the Earth's surface. *Earth and Planetary Science Letters*, **267**, 146–160, <https://doi.org/10.1016/j.epsl.2007.11.040>.

Sætre, C., Hellevang, H., Dennehy, C., Dypvik, H. and Clark, S. 2018. A diagenetic study of intrabasaltic siliciclastics sandstones from the Rosebank field. *Marine and Petroleum Geology*, **98**, 335–355, <https://doi.org/10.1016/j.marpetgeo.2018.08.026>.

Saunders, A.D., Fitton, J.G., Kerr, A.C., Norry, M.J. and Kent, R.W. 1997. The North Atlantic Igneous Province. In: Mahoney, J. and Coffin, M. (eds) *Large Igneous Provinces: Continental*,

- Oceanic, and Planetary Flood Volcanism*. 45–93., <https://doi.org/10.1029/GM100p0045>.
- Schofield, N. and Jolley, D.W. 2013. Development of intra-basaltic lava-field drainage systems within the Faroe-Shetland Basin. *Petroleum Geoscience*, **19**, 273–288, <https://doi.org/10.1144/petgeo2012-061>.
- Schofield, N., Holford, S., et al. 2015. Regional magma plumbing and emplacement mechanisms of the Faroe-Shetland Sill Complex: Implications for magma transport and petroleum systems within sedimentary basins. *Basin Research*, **29**, 41–63, <https://doi.org/10.1111/bre.12164>.
- Schöpfer, K. and Hinsch, R. 2019. Late Palaeozoic – Mesozoic tectonostratigraphic development of the eastern Faroe-Shetland Basin: New insights from high-resolution 3D seismic and well data. *Marine and Petroleum Geology*, **109**, 494–518, <https://doi.org/10.1016/j.marpetgeo.2019.04.007>.
- Schumm, S.A. 1993. River Response to Baselevel Change: Implications for Sequence Stratigraphy. *The Journal of Geology*, **101**, 279–294.
- Shaw Champion, M.E., White, N., Jones, S.M. and Lovell, J.P.B. 2008. Quantifying transient mantle convective uplift: An example from the Faroe-Shetland basin. *Tectonics*, **27**, TC1002, <https://doi.org/10.1029/2007TC002106>.
- Sheriff, R.E. and Geldart, L.P. 1982. *Exploration Seismology Volume 1: History, Theory and Data Acquisition*.
- Sleep, N.H. 1990. Hotspots and mantle plumes: some phenomenology. *Journal of Geophysical Research*, **95**, 6715–6736, <https://doi.org/10.1029/JB095iB05p06715>.
- Smallwood, J.R. and Gill, C.E. 2002. The rise and fall of the Faroe–Shetland Basin: evidence from seismic mapping of the Balder Formation. *Journal of the Geological Society, London*, **159**, 627–630.
- Stoker, M.S., Holford, S. and Hillis, R.R. 2017. A rift-to-drift record of vertical crustal motions in the Faroe – Shetland Basin , NW European margin : establishing constraints on NE Atlantic evolution. *Journal of the Geological Society*, **175**, 263–274.
- Stucky de Quay, G., Roberts, G.G., Watson, J.S. and Jackson, C.A.L. 2017. Incipient mantle plume evolution: Constraints from ancient landscapes buried beneath the North Sea. *Geochemistry, Geophysics, Geosystems*, **18**, 973–993, <https://doi.org/10.1002/2016GC006769>.
- Underhill, J. 2001. Controls on the genesis and prospectivity of Paleogene palaeogeomorphic traps , East Shetland Platform , UK North Sea. *Marine and Petroleum Geology*, **18**, 259–281.
- Walker, F., Schofield, N., Millett, J.M., Jolley, D.W., Hole, M.J. and Stewart, M. 2020. Paleogene volcanic rocks in the northern Faroe–Shetland Basin and Møre Marginal High: understanding lava field stratigraphy. *Geological Society, London, Special Publications*, SP495-2019–13, <https://doi.org/10.1144/SP495-2019-13>.
- Walker, F., Schofield, N., et al. 2021. Inside the volcano: 3D magmatic architecture of a buried shield volcano. *Geology*, **49**, 243–247, <https://doi.org/10.1130/G47941.1/5164801/g47941.pdf>.

- Watson, D., Schofield, N., et al. 2017. Stratigraphic overview of Palaeogene tuffs in the Faroe–Shetland Basin, NE Atlantic Margin. *Journal of the Geological Society*, **174**, 627–645, <https://doi.org/10.1144/jgs2016-132>.
- White, R.S. 1989. Initiation of the Iceland Plume and Opening of the North Atlantic. *In: Extensional Tectonics and Stratigraphy of the North Atlantic Margins*. 149–154.
- White, R.S. and McKenzie, D. 1989. Magmatism at rift zones: The generation of volcanic continental margins and flood basalts. *Journal of Geophysical Research*, **94**, 7685–7729, <https://doi.org/10.1029/JB094iB06p07685>.
- Widess, M.B. 1973. How Thin Is a Thin Bed? *Geophysics*, **38**, 1176–1180, <https://doi.org/10.1190/1.1440403>.
- Wilkinson, C.M., Ganerød, M., Hendriks, B.W.H. and Eide, E.A. 2016. Compilation and appraisal of geochronological data from the North Atlantic Igneous Province (NAIP). *In: Peron-Pinvidic, G., Hopper, J. R., Stoker, M. S., Gaina, C., Doornenbal, J. C., Funck, T. and Arting, U. E. (eds) The NE Atlantic Region: A Reappraisal of Crustal Structure, Tectonostratigraphy and Magmatic Evolution*, <https://doi.org/http://doi.org/10.1144/SP447.10>.
- Ziegler, P.A. 1988. Evolution of the Arctic - North Atlantic and the Western Tethys - A Visual Presentation of a series of Paleogeographic-paleotectonic maps. *AAPG Memoir*, **43**, 164–196.

Tables

Table 1

Survey Name	Acquisition Company	Acquisition Date	Air-gun		Recording Length (ms)	Shot-point Interval (m)	Streamer		Area (km ²)
			No.	Volume (in ³)			No.	Length (m)	
Erlend Basin 2012 Phase 1 (EB12 (1))	TGS	2012	2	4240	8200	18.75	8	6000	3300
Erlend Basin 2012 Phase 2 (EB12 (2))	TGS	2012	2	4100	8000	18.75	12	6000	
DN08	Dong Energy	2008	2	3090	7168	25	16	4800	
DN09	Dong Energy	2009	2	3111	7168	25	16	4800	
MSMB99	Aker	1999	2	3510	7168	25	8	4050	
Brendan Basin 2014 (BB14)	TGS	2014	2	3480	8200	18.75	12	6000	2413
Erlend Mid West 2014 (EMW14)	TGS	2014	2	3480	8200	18.75	12	6000	893
Erlend West 2012 (EW12)	TGS	2012	2	4100	8060	18.75	12	6000	1583

Table 2

Horizon	Seismic character	Confidence
Top Balder Fm.	Mostly high-amplitude but variable in places, positive, largely continuous	Mostly high
Top Basalt	High-amplitude, continuous to semi-continuous, positive	High
Base Basalt	Highly variable amplitude, semi-continuous to discontinuous, negative	Mostly low, but high beneath Erlend Volcano
Flett Unconformity	Variable amplitude (typically high in deep incisions, lower in-between), continuous to semi-continuous, positive. Horizon is commonly extremely irregular	Typically high
Upper Thanetian Unconformity	Moderate to high amplitude, semi-continuous, positive. Commonly merges into the overlying Flett Unconformity	Typically high, where present
Top Cretaceous	High amplitude (outside volcanic cover; low-amplitude to invisible beneath basalt), continuous, positive	High outside volcanic cover, very low beneath basalt

Table 3

Well	Depth of Interest (m)	Wireline Curves Availability					
		Gamma Ray	Caliper	Compressional Sonic	Density	Neutron Porosity	Resistivity
208/15-1a	1450-1550	Y	N	N	N	N	Y
208/15-2	1300-1450	Y	Y	Partial	Y	Y	Partial
209/6-1	1450-1550	Y	N	Y	N	N	Y
209/12-1	1250-1350	Y	N	Partial	N	N	Partial

Table Captions

Table 1. Seismic surveys making up the merged 3D survey Northern Lights used in this study.

Table 2. Seismic characteristics and interpretation confidence for the horizons interpreted in this study.

Table 3. Key wells used in this study, showing the availability of wireline curves for the depth of interest for this study.

Figure Captions

Fig. 1. A) Structural map of the Faroe-Shetland Basin. Black box shows the location of (b). Blue shape shows the location of the seismic dataset used in this study; green shape shows the seismic dataset used by Smallwood & Gill (2002), Shaw Champion et al. (2008) and Hartley et al. (2011) to map the incision surface in the Judd Sub-basin. Yellow circles highlight wells in which the Upper Thanetian Unconformity and/or Flett Unconformity have been recognised, according to Jolley et al. (2021). Base map adapted from Ritchie et al. (2011). B) Close-up map of the study area highlighting wells used for this study and the locations of seismic lines throughout this paper.

Fig. 2. Chart showing the generalised lithological column for the Faroe-Shetland Basin, the lithostratigraphic nomenclature for the FSB (from Ritchie et al., 2011) and how these relate to the T-sequence framework devised by Ebdon et al. (1995). Eustatic sea level curve is taken from Haq and Al-Qahtani (2005), and shows the change in global sea level compared to the present day at 0. UTU = Upper Thanetian Unconformity, FU = Flett Unconformity. Arrows indicate approximate ages of the unconformities/incision surfaces identified in previous studies. The ages of the T-sequences and lithostratigraphic units are taken from the recently-updated timescale of Jolley et al. (2021), and thus differ from previous publications.

Fig. 3. Map highlighting the drainage systems discussed in the text, both from this study and previous studies. The broad geometries and drainage directions of the drainage systems are shown, along with the boundaries of the seismic surveys used to interpret them. Approximate depositional systems for the FSB and surrounding areas adapted from Mudge (2015). Position of line of breakup and Greenland shown for 54 Ma, after Mudge (2015). Judd drainage system from Hartley et al. (2011), Cambo drainage system from Hardman et al. (2018a) and Bressay system from Stucky de Quay et al. (2017).

Fig. 4. RGB frequency spectral decomposition of the Flett Unconformity surface displaying the locations of wells used in this study and seismic lines shown throughout this paper. Basalts of the Erlend High and granitic to gneissic basement of the North Shetland Platform show as very bright amplitudes. Channels of the drainage system are typically displayed as moderate amplitudes, with brightening occurring just downstream of the NSP. Curvilinear features interpreted as paleocoastlines (EI-3 and WI-3) are also highlighted.

Fig. 5. Correlation panel of the four key wells for this study (208/15-2, 208/15-1a, 209/6-1 and 209/12-1). See Figs. 1b and 3. for well locations. Lithologies are interpreted based on a combination of gamma ray and density wireline curves and composite log reports. Sequence boundaries and the positions of the unconformities are defined based on biostratigraphy.

Fig. 6. A) TWT surface of the Flett Unconformity, showing well locations and the edge of the volcanic cover (red dashed line). Channels of the incision surface are annotated, showing the complex geometry of the drainage system, with a large trunk stream flowing westwards between the Erlend Volcano and North Shetland Platform, fed by numerous tributaries sourced from both highs. Note incision into the crest of the NSP. B) Copy of (A), with certain parts of the drainage system colour-coded for clarity. See text for meaning of the colours.

Fig. 7. Seismic line showing the Flett and Upper Thanetian Unconformities incising into sediments in the Flett Sub-Basin and into the top of the North Shetland Platform. Note that the two unconformities are merged on top of the high. See Figs. 1b and 3 for line location.

Fig. 8. Seismic line through the key wells shown in Fig. 5, showing the variation in the FU and UTU across the study area. Note that the two unconformities are merged into a single seismic reflection in 208/15-1a and 209/12-1, and significant separation occurs only in 208/15-2. See Figs. 1b and 3 for location.

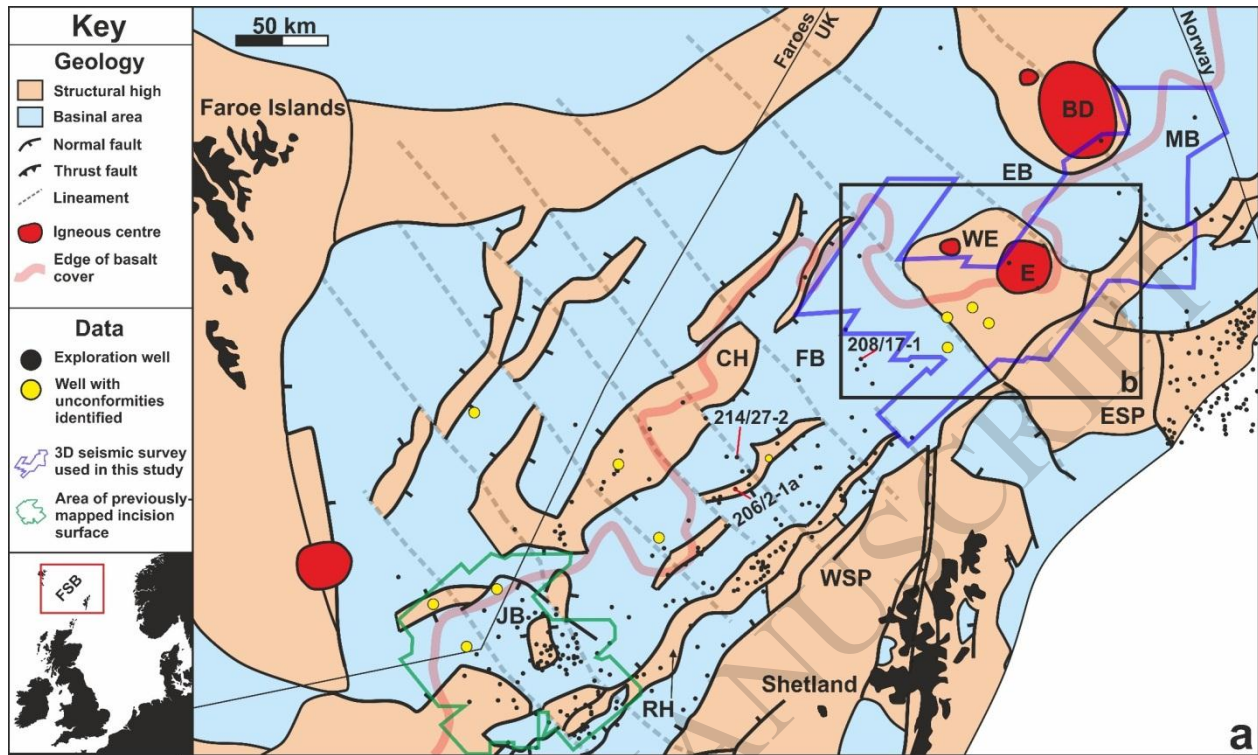
Fig. 9. Seismic line showing the FU and UTU compared to the Erlend Volcano. The UTU is clearly visible incising beneath the FU, and appears to occur between the Lower Volcanic Sequence (forming the Erlend volcanic edifice) and the Upper Volcanic Sequence (post-edifice lava flows), indicating that the volcano formed prior to sequence T40. See Figs. 1b and 3 for line location.

Fig. 10. Seismic line showing interaction between incised channels and forced folds above sill intrusions. The channels preferentially occur at the margins of the folds, indicating that they have been diverted by them. Note the thickness changes of the strata immediately overlying the Top Cretaceous horizon. See Figs. 1b and 3 for line location.

Fig. 11. Seismic line showing the cross-section of the western coastlines shown in Fig. 4. Three ridges are observed, occurring just above the FU and therefore within sequence T45.

Fig. 12. Seismic line showing the cross-section of the eastern coastlines shown in Fig. 4. The coastlines highlighted by the brightness changes on the spectral decomposition in Fig. 4 appear to correspond to onlapping of sequence T45-50 sediments onto the Flett Unconformity surface.

Figure 1



- BD: Brendans Dome Volcanic Centre
- CH: Corona High
- EB: Erlend sub-basin
- ESP: East Shetland Platform
- EV: Erlend Volcano
- FB: Flett sub-basin
- FSB: Faroe-Shetland Basin
- JB: Judd sub-basin
- MB: Møre Basin
- RH: Rona High
- WE: West Erlend Volcanic Centre
- WSP: West Shetland Platform

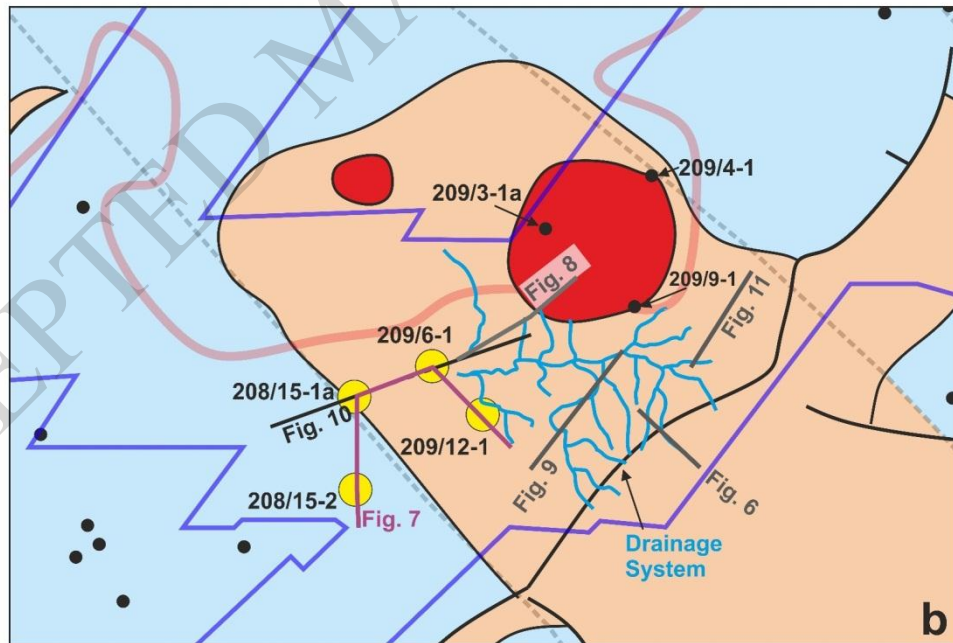
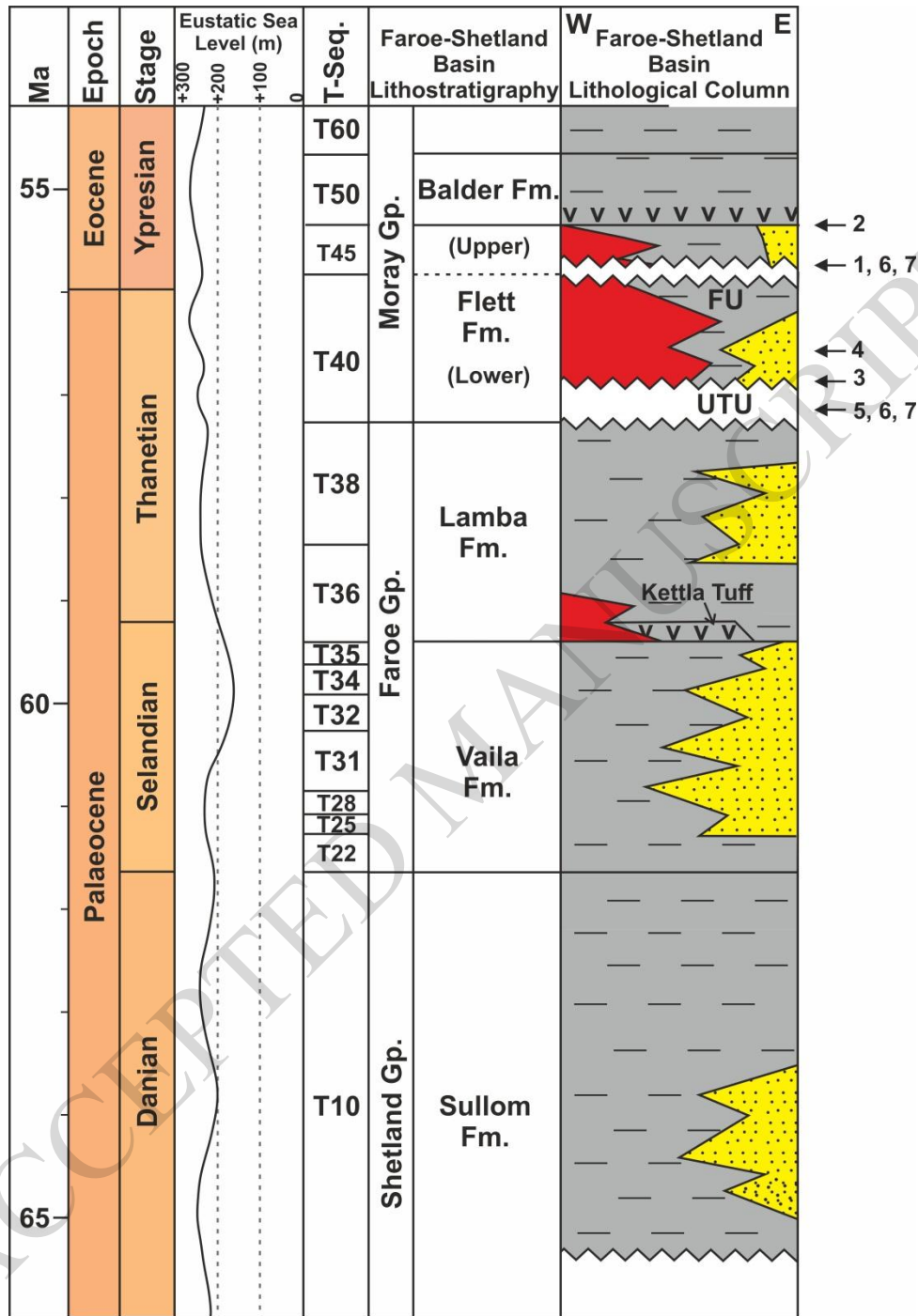


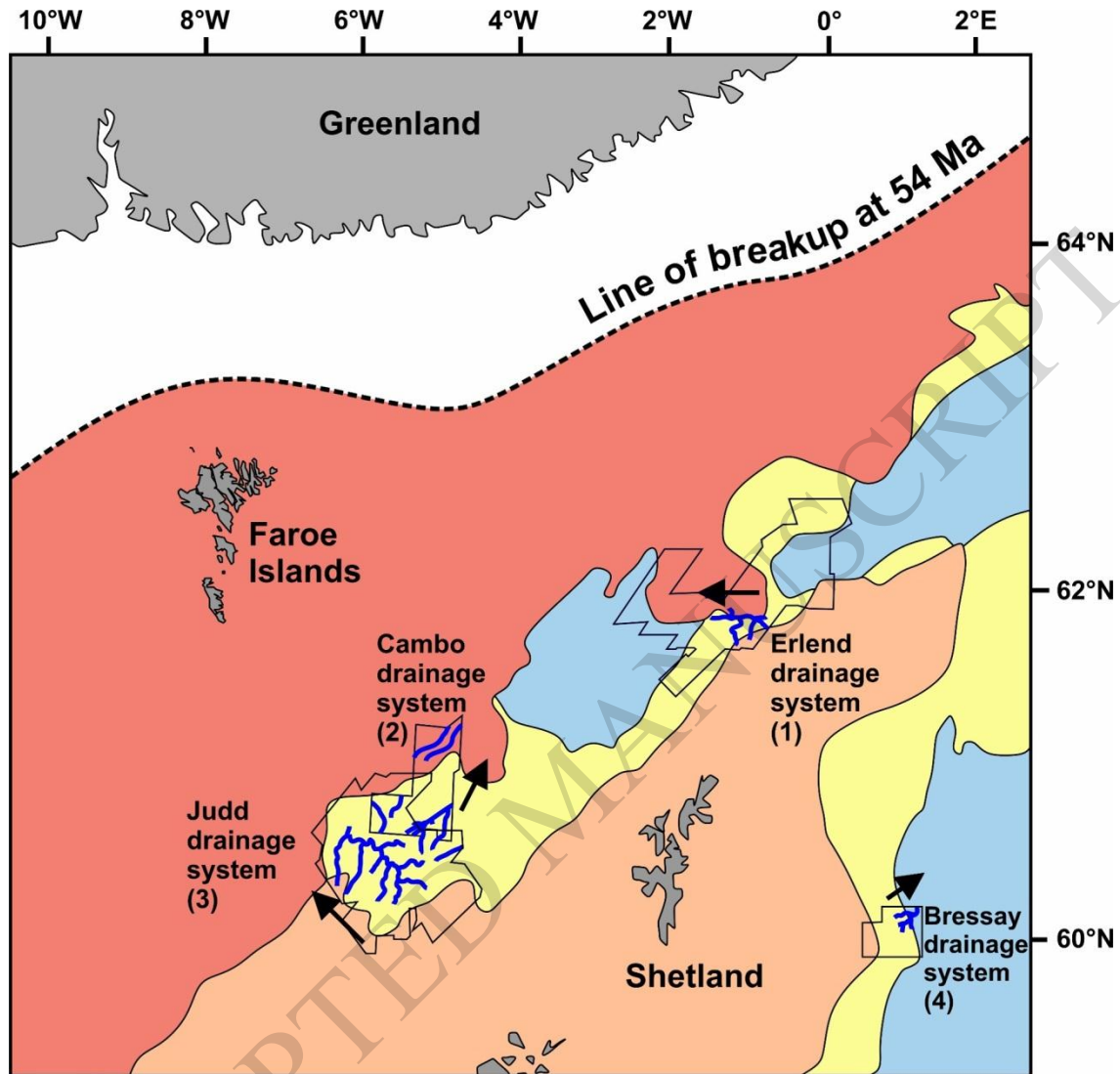
Figure 2



Mud-dominated
 v = tuffaceous
 Sand-dominated
 Basalt

- 1: Underhill (2001)
- 2: Smallwood and Gill (2002)
- 3: Shaw Champion *et al.* (2007)
- 4: Hartley *et al.* (2011)
- 5: Stucky de Quay *et al.* (2017)
- 6: Hardman *et al.* (2018)
- 7: Jolley *et al.* (2021)

Figure 3



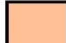




	Exposed land	<ol style="list-style-type: none">1. This study2. Hardman <i>et al.</i> (2018a)3. Smallwood & Gill (2002) Shaw Champion <i>et al.</i> (2008) Hartley <i>et al.</i> (2011) Jolley <i>et al.</i> (2021)4. Underhill (2001) Stucky de Quay <i>et al.</i> (2017)
	Non marine and continental shelf	
	Basin	
	Volcanic cover	
	Seismic surveys and mapped drainage systems	

Figure 4

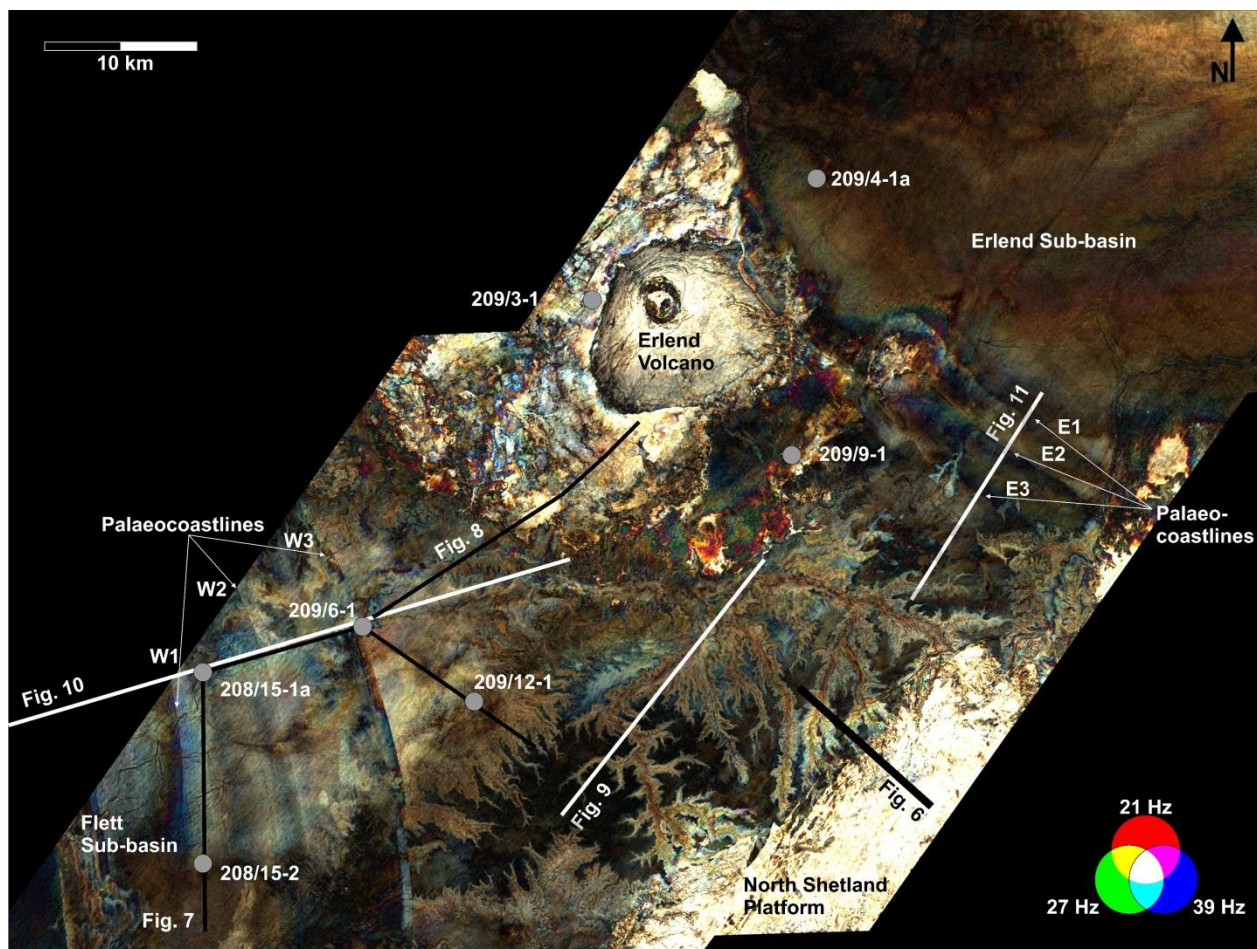


Figure 5

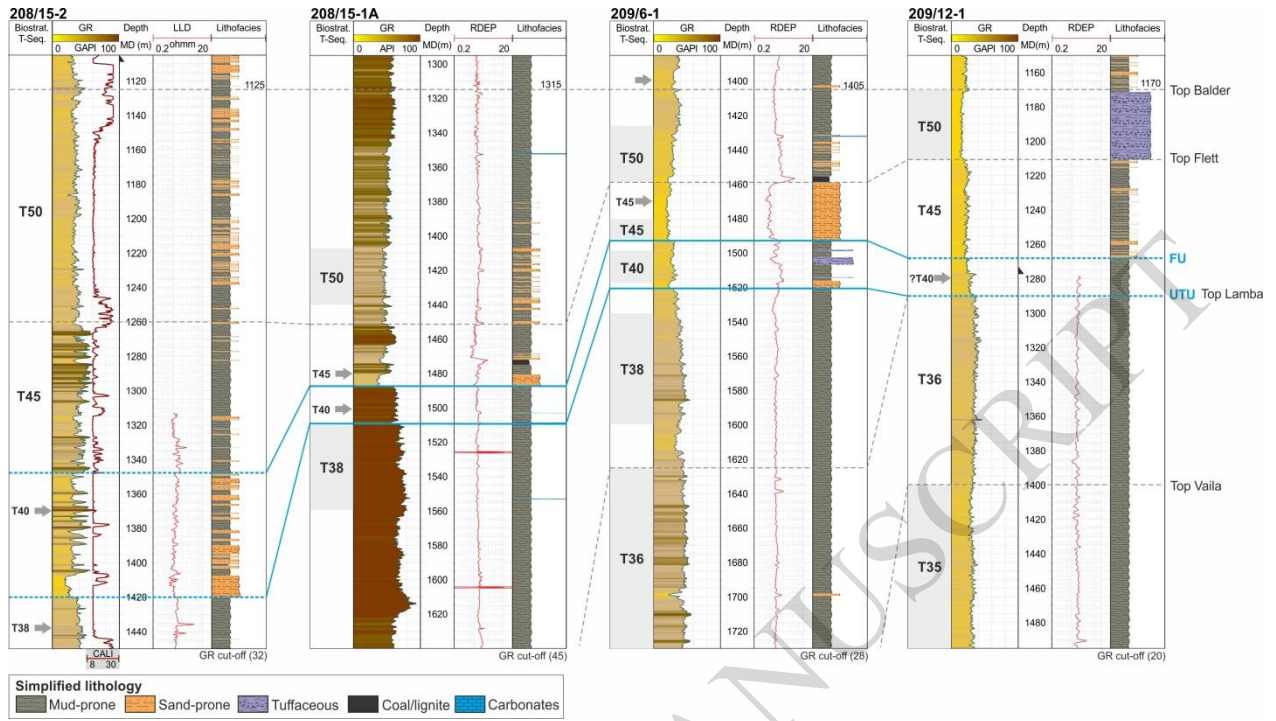


Figure 6

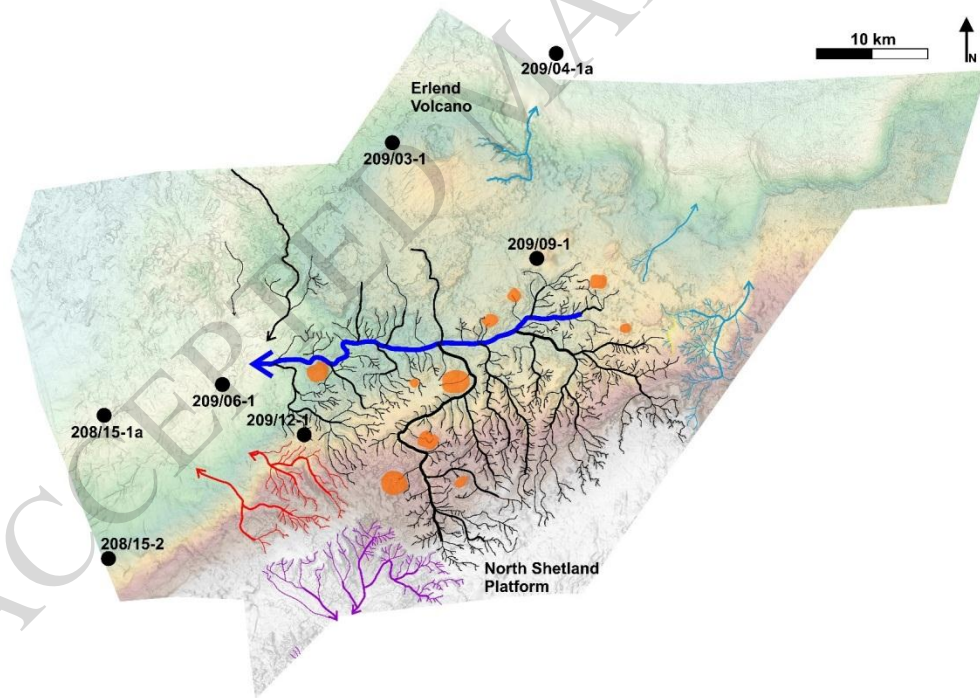
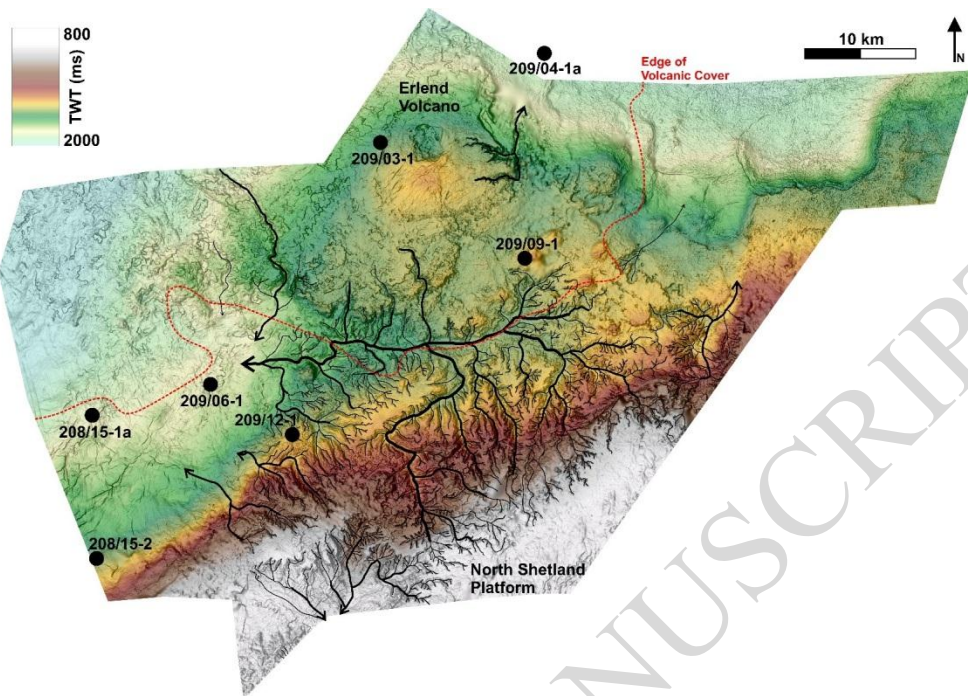


Figure 7

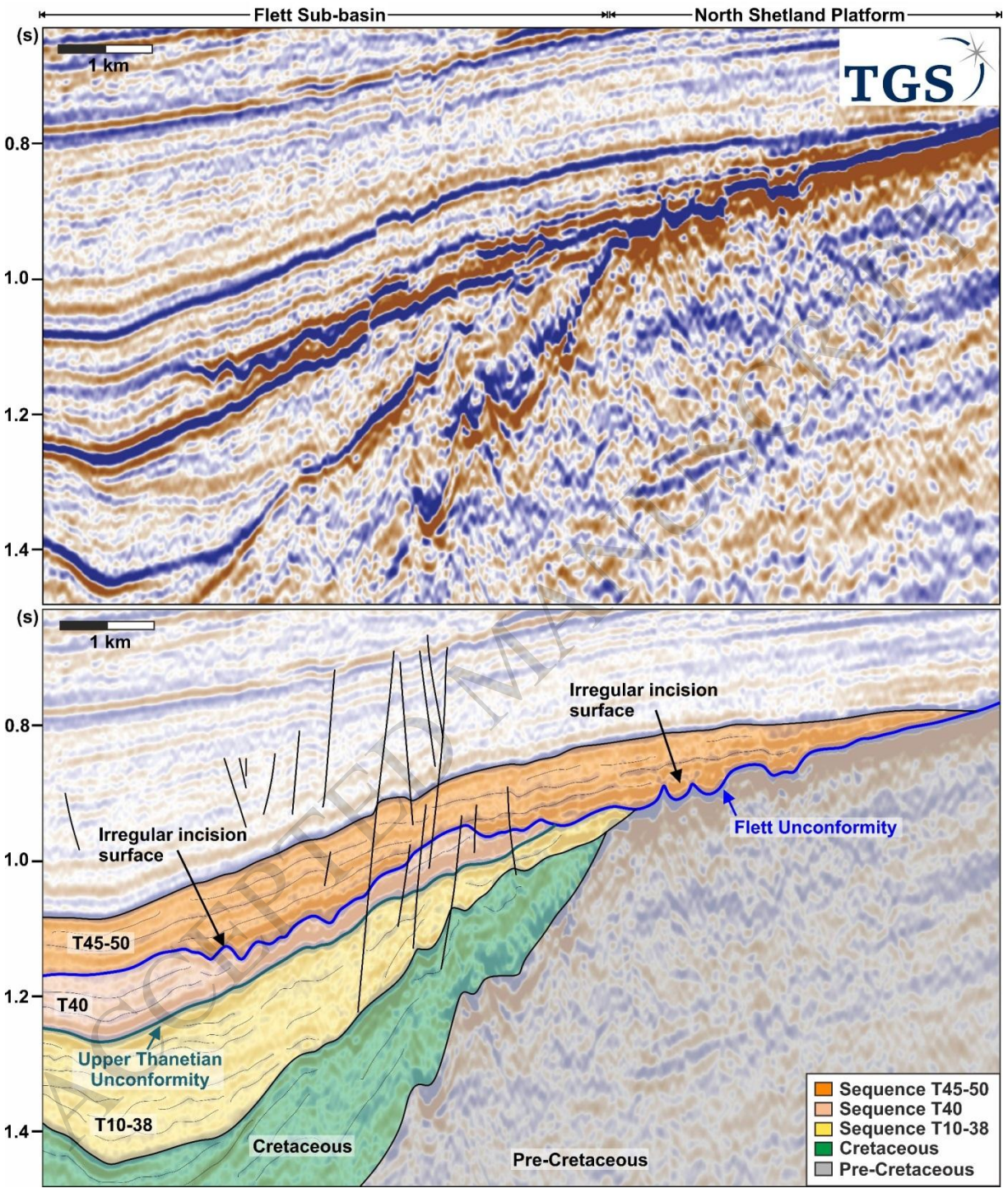
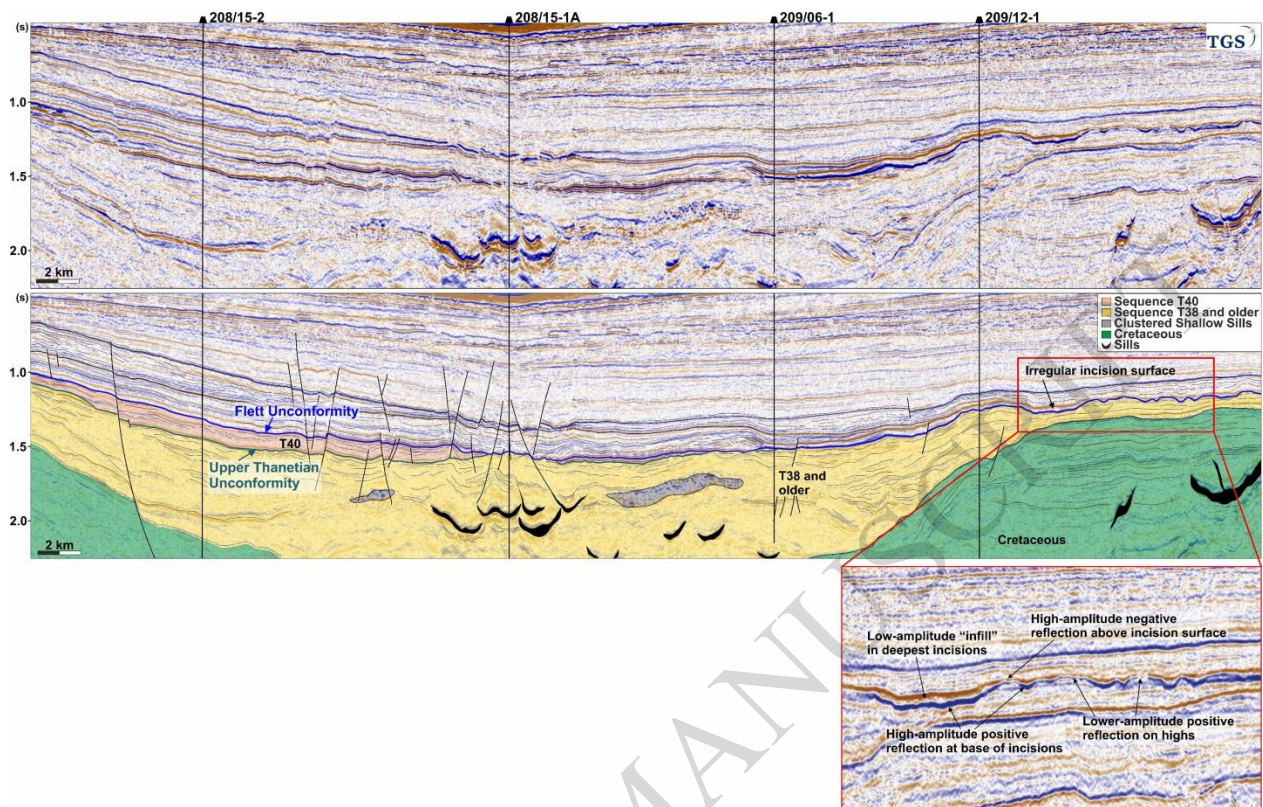


Figure 8



ACCEPTED MANUSCRIPT

Figure 9

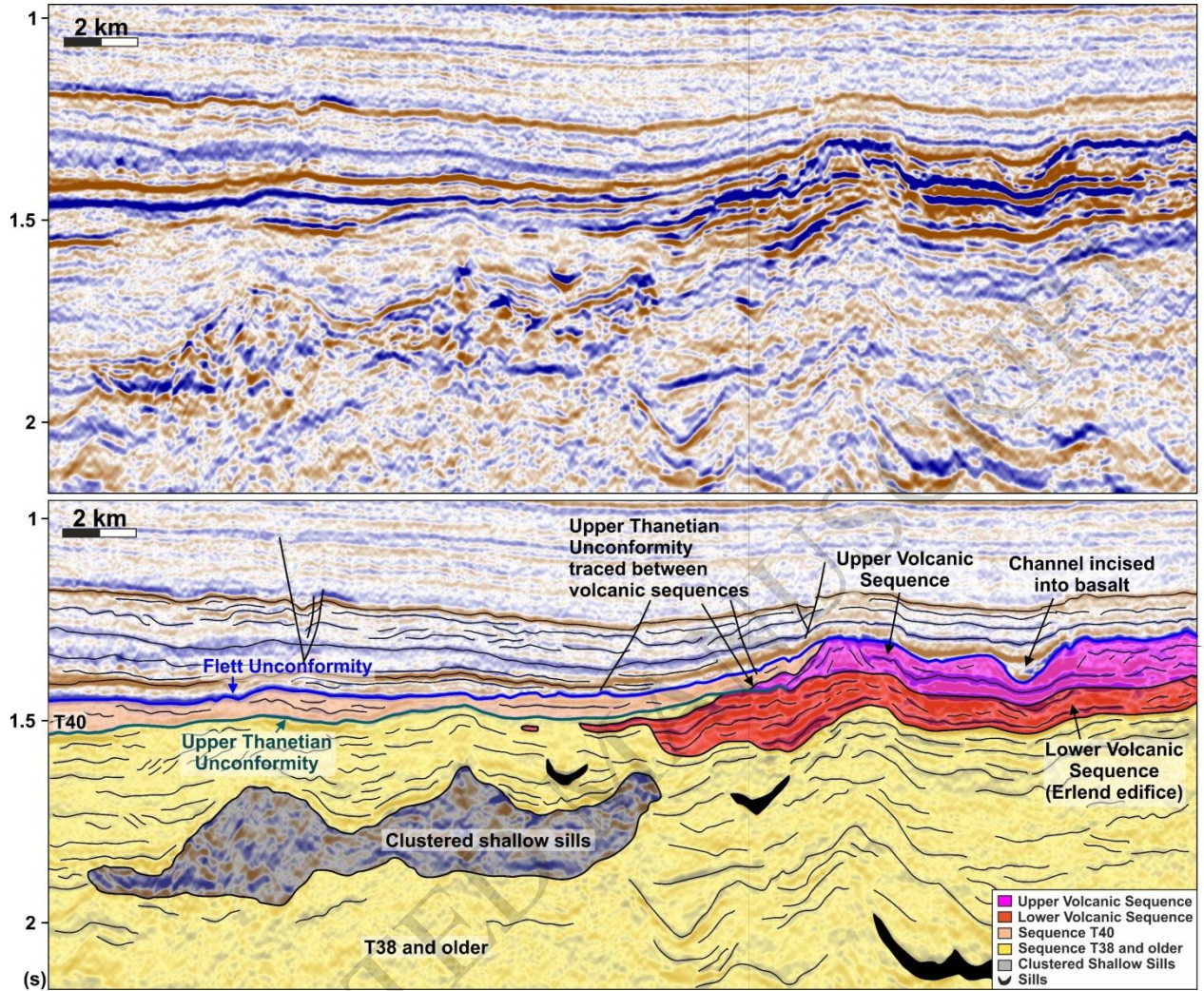


Figure 10

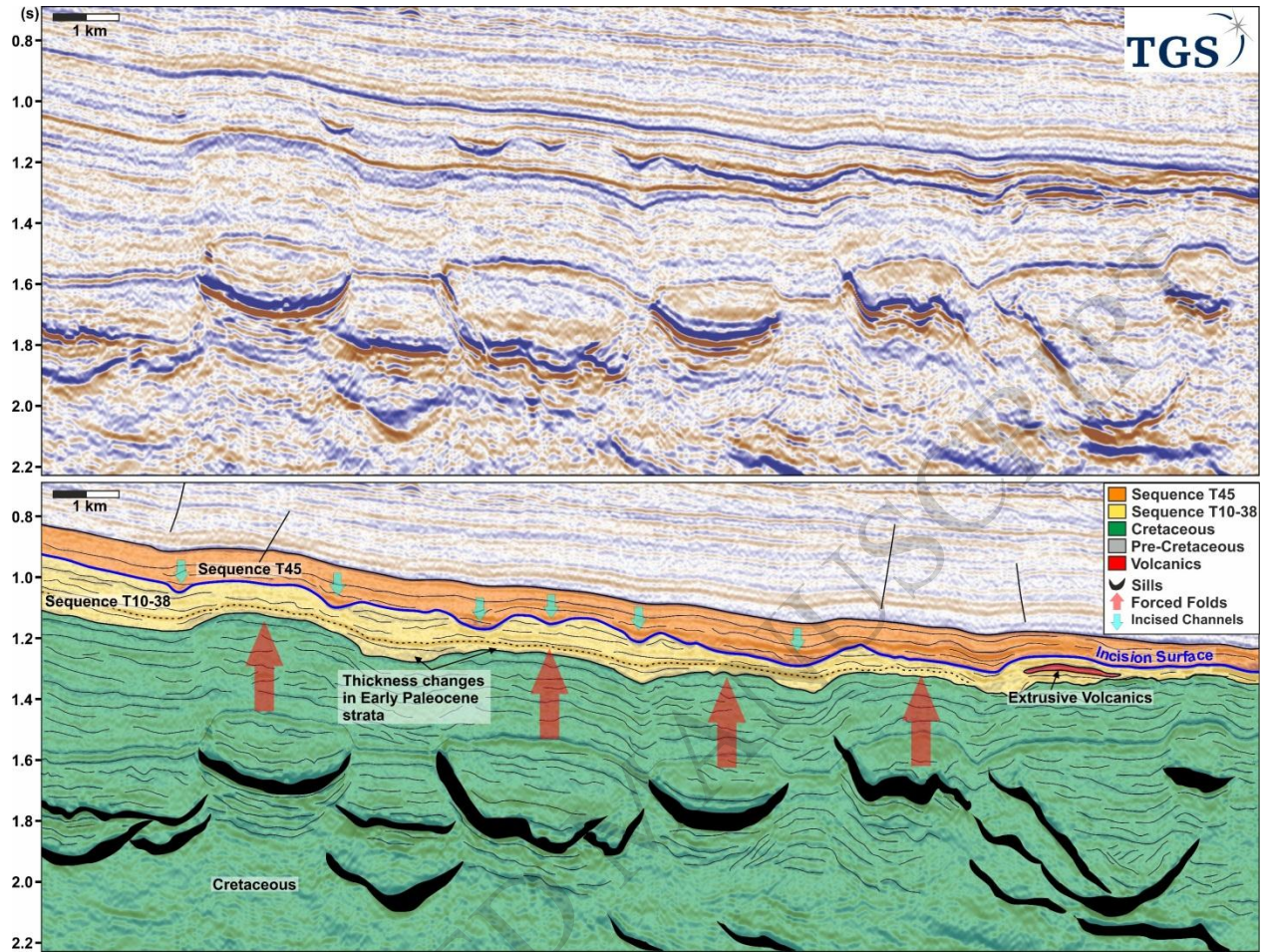


Figure 11

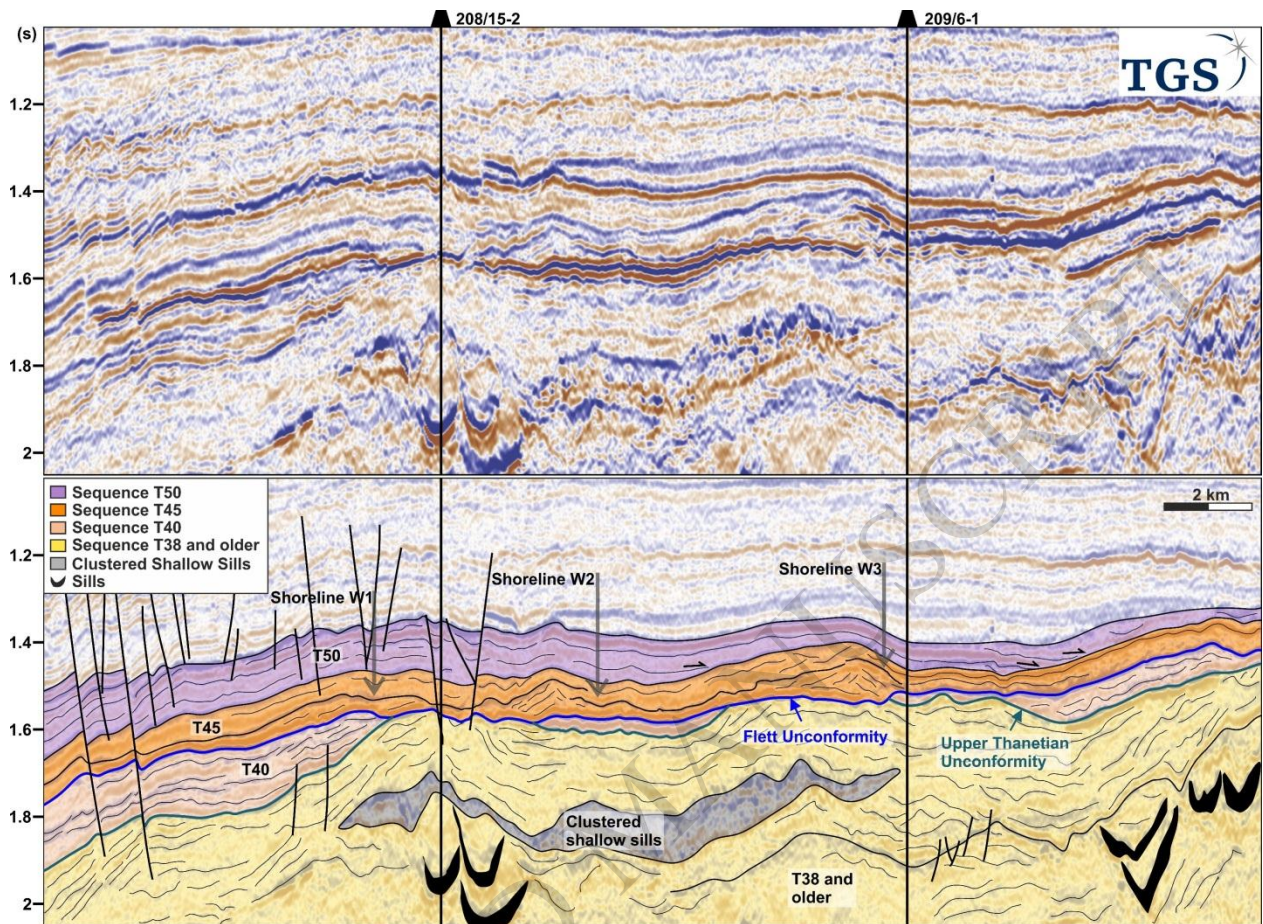


Figure 12

